NATIONAL ADVISORY COMMITTEE FOR AERONAUTICS

TECHNICAL NOTE 3479

ANALYSIS OF THE HORIZONTAL-TAIL LOADS MEASURED IN FLIGHT ON A MULTIENGINE JET BOMBER

By William S. Aiken, Jr., and Bernard Wiener

Langley Aeronautical Laboratory
Langley Field, Va.

Washington
September 1955

CONTENTS

NATIONAL ADVISORY COMMITTEE FOR AERONAUTICS

TECHNICAL NOTE 3479

ANALYSIS OF HORIZONTAL-TAIL LOADS MEASURED IN FLIGHT ON A MULTIENGINE JET BOMBER

By William S. Aiken, Jr., and Bernard Wiener

SUMMARY

Horizontal-tail loads were measured in gradual and abrupt longitudinal maneuvers on two configurations of a four-engine jet bomber. The results obtained have been analyzed to determine the flight values of the coefficients important in calculations of horizontal-tail loads. The least-squares procedure used to determine aerodynamic tail loads from strain-gage measurements of structural tail loads which were affected by temperature is covered in detail. The effect of fuselage flexibility on the airplane motion is considered in the analysis of the abrupt-maneuver data. When possible, wind-tunnel results are compared with flight results. Some calculations of critical horizontal-tail loads beyond the range of the tests are given and compared with design loads.

INTRODUCTION

Although the factors which make up the horizontal-tail loads have been known for some time, it is customary to reexamine the adequacy of the accepted analytical procedures on airplanes which represent departures in either speed range, size, flexibility, or configuration from previous aircraft on which experience exists. The introduction of the jet-engine bomber represented one such departure since a large change in speed range along with increased flexibility effects were immediately introduced. It was primarily for these reasons that the NACA initiated a program of loads measurement on a North American B-45A airplane. Flight tests were conducted on two configurations of the North American B-45A airplane, configuration A being the original version and configuration B being a modified version having reflexed flaps and other changes.

The primary objectives of the present paper are to report the horizontal-tail-loads measurements for configuration B which have not previously been reported and to summarize the horizontal-tail-loads results obtained with both configurations. The manner in which the

aerodynamic-loads data were analyzed to include structural temperature effects and fuselage flexibility effects constitutes an important part of the present paper. Other objectives of the present paper are the comparison of configuration A flight data with available wind-tunnel results and the presentation of some calculations of critical tail loads for configuration B in pitching maneuvers within the design V-n diagram which are compared with design horizontal-tail loads.

SYMBOLS

Δa_t	tail incremental normal acceleration defined by equation (28), ft/sec^2
$\bar{c}$	wing mean aerodynamic chord, in.
C_{N_A}	airplane normal-force coefficient, nW/qS
$C_{N_{wf}}$	wing-fuselage normal-force coefficient
$C_{m_{\bar{c}/4}}$	pitching-moment coefficient about the quarter chord
$C_{m_{O_m}}$	zero-lift wing-fuselage pitching-moment coefficient calculated from L_{t_O}
$C_{m_{O_c}}$	$C_{m_{O_m}}$ corrected for area, elevator angle, and thrust
C_{m_O}	zero-lift wing-fuselage pitching-moment coefficient ($C_{m_{O_c}}$ including additional corrections for errors due to structural temperature effects on measured tail loads)
d	distance from wing-fuselage aerodynamic center to airplane center of gravity, negative rearward, in.
$d_{.277}$	distance from wing-fuselage aerodynamic center to a center-of-gravity location at $0.277\bar{c}$, negative rearward, in.
g	acceleration of gravity, ft/sec^2
h_p	pressure altitude, ft
I_y	airplane pitching moment of inertia, $slug\text{-}ft^2$

k_y	airplane radius of gyration in pitch, ft
l_e	effective distance of M_e from center of gravity, negative rearward, in.
l_m	distance from center of gravity of airplane to center of gravity of W_{tf}, negative rearward, in.
l_n	distance between nose linear accelerometer and center-of-gravity linear accelerometer, in.
l_t	distance from airplane center of gravity to tail quarter chord, rearward negative (for center of gravity at 27.7 percent $\bar{c}$, l_t = -397.5 in.), in.
L_t	aerodynamic tail load, lb
L_{t_M}	measured aerodynamic tail load, lb
L_{t_0}	aerodynamic tail load at zero load factor, lb
$L_{t_{SM}}$	measured structural tail load, lb
$L_{t_{.277}}$	aerodynamic tail load with center of gravity at reference condition (27.7 percent $\bar{c}$), lb
M	Mach number
M_e	effective mass of tail-fuselage combination, slugs
n	load factor at center of gravity
n_{high}	a maximum center-of-gravity load factor
n_{low}	a minimum center-of-gravity load factor
n_n	load factor at nose
n_t	load factor at tail
q	dynamic pressure, lb/sq ft
S	wing area, sq ft

s	standard error of estimate
T	total engine thrust, lb
ΔT	average difference in structural temperatures, ground to flight, $^{\circ}F$
V_L	left horizontal tail shear, lb
V_R	right horizontal tail shear, lb
W	airplane weight, lb
W_t	weight of horizontal-tail assembly, lb
W_{t_o}	weight of horizontal tail outboard of strain-gage station, lb
W_{tf}	weight of tail assembly and fuselage behind wing rear spar, lb
x_{ac}	location of wing-fuselage aerodynamic center, percent $\bar{c}$
x_{ac_m}	wing-fuselage aerodynamic-center position uncorrected for area and elevator angle per g, percent $\bar{c}$
x_{cg}	location of airplane center of gravity, percent $\bar{c}$
x_t	distance from wing-fuselage aerodynamic center to horizontal-tail quarter chord, negative rearward, $l_t + d$, in.
δ_e	effective elevator angle, negative up, deg
δ_{e_o}	elevator angle at zero airplane load factor, deg
ϵ	error of fit (with subscripts to identify particular parameter considered)
$\ddot{\theta}_{cg}$	pitching acceleration at center of gravity, radians/sec^2
$\ddot{\theta}_r$	pitching acceleration defined by equation (27), radians/sec^2
$\ddot{\theta}_t$	pitching acceleration defined by equation (24), radians/sec^2
ρ_{M_L}	nondimensional left moment bridge output

ρ_{M_R} nondimensional right moment bridge output

ρ_{V_L} nondimensional left shear bridge output

ρ_{V_R} nondimensional right shear bridge output

APPARATUS AND TESTS

AIRPLANE

Two configurations of the North American B-45A airplane were used for this investigation. For purposes of identification herein, the original configuration is designated configuration A and the service configuration incorporating reflexed flaps and other changes is designated configuration B. A side view of the airplane is shown in figure 1 and pertinent characteristics are presented in table I. A two-view line drawing of the airplane is shown in figure 2(a), and the wing trailing-edge contours of the two configurations are compared in figure 2(b). The bent-down trailing-edge strip also shown in figure 2(b) increased the wing area slightly, but all coefficients computed for configuration B are with respect to the original wing area. In addition to the reflexed flap, the ailerons were uprigged 3.8° and end plates were added to the flap-fuselage and flap-nacelle junctures. The tip of the horizontal tail outboard of the elevator was modified by a 2° downward bend of the trailing edge rearward of the rear spar.

INSTRUMENTATION

Instrumentation pertinent to the present paper consisted of standard NACA recording instruments used to measure airspeed and altitude, normal accelerations at the nose (for tests of configuration B), at the center of gravity, and at the tail, pitching velocities and pitching accelerations at the center of gravity and the tail, and elevator control positions.

An airspeed boom was mounted at the left wing tip with the airspeed head approximately 1 local chord ahead of the leading edge of the wing. The results of a flight calibration of the airspeed system for position error and an analysis of available data for a similar installation indicate that the measured Mach number differed from the true Mach number by less than ± 0.01 throughout the test range.

Fuselage skin temperatures were measured at four locations on the aft portion of the fuselage (approximate locations shown in figure 2(a)) by use of Stikon gages with outputs recorded on an 18-channel oscillograph.

Electrical wire-resistance strain gages (Type A-6 with low temperature correction factors), installed as four-active-arm bridges on the main spars of the left and right sides of the horizontal tail approximately 8 percent of the tail semispan outboard of the airplane center line, were used for measuring the left and right tail root shears and bending moments.

The strain-gage-bridge installation was calibrated according to the method detailed in reference 1. The bridges were then combined electrically so that, except for secondary carryover effects, a combined shear or bending-moment bridge responded primarily to shear or to bending moment for the side of the tail on which the load was being measured. The final calibration equations which were used to determine the left and right side shears in evaluating flight horizontal-tail loads were

$$\begin{Bmatrix} V_L \\ V_R \end{Bmatrix} = \begin{bmatrix} 6{,}845 & 295 & 0 & 680 \\ 0 & 705 & 4{,}790 & 0 \end{bmatrix} \begin{Bmatrix} \rho_{V_L} \\ \rho_{M_L} \\ \rho_{V_R} \\ \rho_{M_R} \end{Bmatrix} \tag{1}$$

where V_L and V_R are the measured loads and ρ_{V_L}, ρ_{M_L}, and so forth are defined as

$$\rho = \frac{\text{Flight deflection - Ground zero deflection}}{\text{Calibrate signal deflection}} \tag{2}$$

The combined strain-gage outputs were recorded on an 18-channel oscillograph with individual galvanometer responses flat to 60 cps. All data were evaluated by using the nondimensional deflections ρ and by recording the sensitivity of each combined bridge immediately prior to a maneuver through the use of a calibrate signal. With this system of data reduction, fluctuations in battery voltage had no effect on the measurement of loads. In addition, galvanometer zeros with strain-gage power off were taken for each run, and thus mechanical shifts in the galvanometer zero position due to temperature effects in the recorder and any thermal electromotive-force effects in the strain-gage circuits were compensated. The resulting accuracy for total structural tail-loads measurement was $\pm$200 pounds.

TESTS

All tests were made with the airplane in the clean condition for both configurations A and B. For configuration A, gradual turn maneuvers were made at altitudes of approximately 15,000, 22,500, 30,000 and 35,000 feet, and abrupt pitching maneuvers were made at 20,000 feet with airplane weights between 52,900 and 63,600 pounds and with centers of gravity between 27.0 and 29.7 percent $\bar{c}$. For configuration B, gradual turn maneuvers were also made at 15,000, 22,500, 30,000, and 35,000 feet and abrupt pitching maneuvers at 20,000 feet with airplane weights between 55,100 and 64,100 pounds and with centers of gravity between 27.2 and 28.2 percent $\bar{c}$.

Table II is a summary of the flight tests reported in the present paper. The configuration, type of maneuver, flight and run number, test altitude, average Mach number, average dynamic pressure, airplane weight, and center-of-gravity position are listed. The gradual turn maneuvers were made at low rates of elevator motion, and the resulting airplane pitching accelerations were, for all practical purposes, zero so that data obtained in these maneuvers can be considered to be trim values at various values of normal acceleration. Mach number and altitude changes during any maneuver were small.

RESULTS AND DISCUSSION

In the following sections are presented (a) the results and analysis of the gradual maneuvers for both configurations, (b) the results and analysis of abrupt pitching maneuvers for both configurations, (c) a comparison of wind-tunnel data and flight data for configuration A, and (d) the calculation of total horizontal-tail loads for critical conditions for configuration B based on flight data and compared with design limits.

All flight horizontal-tail-loads data presented herein were obtained by using equation (1) to evaluate the shear on the left and right side of the tail. The measured structural tail load is thus defined by the equation

$$L_{t_{SM}} = V_L + V_R \tag{3}$$

The aerodynamic tail load is given by the equation

$$L_{t_M} = L_{t_{SM}} + (n_t - 1)\ W_{t_o} \tag{4}$$

GRADUAL MANEUVERS

Basic Data

Since the gradual maneuvers were made at essentially constant Mach number and altitude and the pitching accelerations were small enough to be considered zero, an equation for balancing tail loads at each instant during any gradual maneuver, taking moments about the wing-fuselage aerodynamic center, may be written as

$$L_t = -\frac{C_{m_0} q S \bar{c}}{x_t} + \frac{nWd}{x_t} \tag{5}$$

For the case where the aerodynamic tail load has a linear relationship to n, the load factor at the center of gravity, equation (5) may be rewritten in the form

$$L_{t_M} = L_{t_0} + \frac{dL_t}{dn} n \tag{6}$$

where L_{t_0} is the aerodynamic tail load at $n = 0$ and $\frac{dL_t}{dn}$ is the slope of the line through plots of tail load against n. From equations (5) and (6) and the following definition

$$x_t = l_t + d \tag{7}$$

a zero-lift pitching-moment coefficient and an aerodynamic-center distance may be obtained from the measured data as

$$C_{m_{0_m}} = \frac{-L_{t_0} x_t}{q S \bar{c}} \tag{8}$$

$$d = \frac{\frac{dL_t}{dn} l_t}{W - \frac{dL_t}{dn}} \tag{9}$$

Configuration A.- For all of the gradual maneuvers listed in table II(a) for configuration A the tail load was plotted against load factor n. Sample plots for six representative runs are shown in figure 3; also shown in figure 3 are plots of effective elevator angle corresponding to the load factor. The effective elevator angle δ_e shown is the average of measurements of elevator angle at the root and

tip of both elevators. The lines shown in figure 3 represent least-squares fittings of straight lines to either the L_{t_M} or δ_e data, while the points are the measured values.

The data shown in figure 3 are for Mach numbers of approximately 0.47 and 0.72 at altitudes of 15,000, 22,500, and 30,000 feet. At $M = 0.47$ at 15,000 feet both δ_e and L_{t_M} may be adequately represented as linear functions of n. For $M = 0.47$ at 22,500 feet the curve for tail load against n cannot be adequately represented by a single straight line but may be represented by two straight lines. The increase in slope occurring at $n = 1.65$ indicates a forward shift in the wing-fuselage aerodynamic center. Other occurrences of breaks or changes in slope of the tail-load curves may be noted for $M = 0.48$ at 30,000 feet and $M = 0.72$ at 30,000 feet.

Inspection of all the data for the gradual maneuvers for configuration A indicated that the forward shift in aerodynamic-center position occurred at a particular airplane normal-force coefficient which varied with Mach number. A summary of the airplane normal-force coefficients defining this shift is shown in figure 4 as a function of Mach number. Three different symbols are used to define the C_{N_A} values; the points shown as circles represent the C_{N_A} corresponding to the intersection of two straight lines passed through the data for L_{t_M} against n as in figure 3 for $M = 0.48$ at 30,000 feet. The points shown as triangles indicate either a maximum C_{N_A} reached without obtaining the break as in figure 3 for $M = 0.47$ at 15,000 feet or a minimum C_{N_A} reached for data which was considered to be above the break boundary.

The tail-loads data below the break were classified as the "lower" C_{N_A} range and data above the break as the "upper" C_{N_A} range; least-squares straight lines of the form of equation (6) were fitted to each run for both upper and lower C_{N_A} ranges where necessary. The distance d between the aerodynamic center and the center of gravity was computed by using $\frac{dL_t}{dn}$ values in equation (9). The aerodynamic-center position determined directly from measurements is defined, in percent $\bar{c}$, as

$$x_{ac_m} = x_{cg} + \frac{d}{\bar{c}} \times 100 \tag{10}$$

A zero-lift pitching-moment coefficient $C_{m_{O_m}}$ was computed by use of L_{t_O} values in equation (8). The x_{ac_m} values and $C_{m_{O_m}}$ values are

listed in table III(a) for the lower C_{N_A} range and in table III(b), for the upper C_{N_A} range along with the run number, pressure altitude, and Mach number.

For subsequent analysis and the determination of tail-off pitching-moment parameters, the following corrections were made to $C_{m_{O_m}}$ and to x_{ac_m}:

(1) For area included between strain-gage stations, $\Delta C_{m_{O_{area}}}$

(2) For elevator-angle-produced tail pitching moment, $\Delta C_{m_{O_\delta}}$

(3) For thrust-produced pitching moment, $\Delta C_{m_{O_{thrust}}}$

(4) For area included between strain-gage stations, $\Delta x_{ac_{area}}$

(5) For elevator-angle-produced tail pitching moment, Δx_{ac_δ}

The following equations were used to compute corrected values of $C_{m_{O_c}}$ and x_{ac}:

$$C_{m_{O_c}} = C_{m_{O_m}} + \Delta C_{m_{O_{area}}} + \Delta C_{m_{O_\delta}} + \Delta C_{m_{O_{thrust}}} \tag{11}$$

or, with numerical values inserted,

$$C_{m_{O_c}} = C_{m_{O_m}} + 0.139 C_{m_{O_m}} + \frac{0.001038\delta_O}{\sqrt{1 - M^2}} - (0.51 \times 10^{-4})\frac{T}{q}$$

and

$$x_{ac} = x_{ac_m} + \Delta x_{ac_{area}} + \Delta x_{ac_\delta} \tag{12}$$

or

$$x_{ac} = x_{ac_m} + 13.9\,\frac{d}{\bar{c}} - 121\,\frac{\dfrac{q}{\sqrt{1 - M^2}}\dfrac{d\delta}{dn}}{W - \dfrac{dL_T}{dn}}$$

In equations (11) and (12) the area correction was based on the assumption that the load between the strain-gage stations would be proportional to the included tail area. The elevator-angle correction terms were based on an assumed value of $\frac{dC_m}{d\delta}$ of $\frac{0.5}{\sqrt{1 - M^2}}$ per radian.

The Glauert factor was used up to $M = 0.70$ and a constant value of 1.4 was used for Mach numbers above 0.70. Thrust was calculated from engine rotational speed and temperature, pressure, and airspeed measurements.

The individual corrections outlined in equations (11) and (12) are listed in table III for all runs. The corrected values of the aerodynamic-center position x_{ac} and zero-lift pitching-moment coefficient $C_{m_{O_c}}$ are given in columns (7) and (12) of this table.

Configuration B.- Sample plots of δ_e and L_{t_M} against n are given for configuration B in figure 5 and represent runs with similar conditions of Mach number and altitude as those illustrated in figure 3 for configuration A. The data shown for $M = 0.48$ and $M = 0.72$ at 30,000 feet indicate definite breaks in L_{t_M} against n. The normal-force coefficients defining the shift in aerodynamic center for configuration B are plotted against Mach number in figure 6. A comparison of figures 4 and 6 indicates that the aerodynamic-center shift occurs at approximately the same combinations of C_{N_A} and M for both configurations.

As with configuration A, the data for configuration B were split into two C_{N_A} ranges, upper and lower. Measured values of $C_{m_{O_m}}$ and x_{ac_m} obtained by equations (8) and (10) were determined for all runs and are listed in table IV(a) for the lower C_{N_A} range and in table IV(b) for the upper C_{N_A} range. Equations (11) and (12) were again used to correct the measured $C_{m_{O_m}}$ and x_{ac_m} values for area between the strain-gage stations, elevator angle, and thrust. The corrections and the corrected values for $C_{m_{O_c}}$ and x_{ac} are listed in table IV(a) for the lower C_{N_A} range and in table IV(b) for the upper C_{N_A} range.

Analysis for Configuration A

The data presented in columns (7) and (12) of table III could normally be used for a direct comparison of flight tail-off and wind-tunnel tail-off pitching-moment characteristics of the test airplane. It became evident, however, that considerable scatter existed in values of $C_{m_{O_c}}$ and x_{ac} for constant Mach numbers at the various test altitudes. Some of this scatter could be attributed to the limited range of data available in a given gradual maneuver before the break or aerodynamic-center shift occurred. Attempts to use plots of $C_{m_{O_c}}$ and x_{ac} against Mach number for the purpose of fairing lines through the data would require consideration of the reliability of each point.

Although such reliability parameters could be established, it would still be difficult to draw a faired curve through points having various values of reliability.

The reliability of the aerodynamic-center position (determined from the slope of the data) for any one maneuver is also a function of the accuracy of the tail-load measurement and the range of load factor covered. The reliability of any one value of $C_{m_{O_c}}$ (determined from the intercept of the straight line through the data) is a function of measurement accuracy, range of load factor, and the amount of extrapolation required. A method of least squares was therefore adopted by which the variation of C_{m_O} and x_{ac} with Mach number could be evaluated and which would weight the data from each run on the basis of load-factor range and extrapolation required.

Lower C_{N_A} range.- In this least-squares procedure for the lower C_{N_A} range, each run was represented by two values of tail load corrected to an average x_{cg} of 27.7 percent $\bar{c}$, one corresponding to the lowest value of load factor for the particular maneuver ($L_{t_{.277}}$ for n_{low}), the other to the highest load factor or break point ($L_{t_{.277}}$ for n_{high}) as

$$\left.\begin{aligned} L_{t_{.277}} &= \frac{-C_{m_{O_c}} qS\bar{c}}{l_t + d} + \frac{n_{low}\, Wd}{l_t + d} && n_{low} \\ L_{t_{.277}} &= \frac{-C_{m_{O_c}} qS\bar{c}}{l_t + d} + \frac{n_{high}\, Wd}{l_t + d} && n_{high} \end{aligned}\right\} \quad (13)$$

Tail loads were thus obtained for comparable center-of-gravity conditions with corrections included for area between strain-gage stations, elevator-angle-induced tail pitching moments, and thrust-induced pitching moments. The values of $C_{m_{O_c}}$ used in equations (13) to compute the tail load corresponds to the data shown in table III(a). The values for d used in equations (13) were calculated from the x_{ac} values given in table III(a) and the selected center-of-gravity position of 27.7 percent $\bar{c}$.

For the least-squares process a form of the equation for fitting the data must be established. The aerodynamic-center position appeared to have a linear variation with Mach number to M = 0.72. The zero-lift pitching-moment coefficient was assumed to vary to this same Mach number as $1/\sqrt{1 - M^2}$, the Glauert factor. The following equation in which moments about the center of gravity are used indicates the form that

was set up from consideration of the assumed C_{m_0} and x_{ac} variations with Mach number:

$$L_{t_{.277}} = -C_{m_0} \frac{q}{\sqrt{1 - M^2}} \frac{S\bar{c}}{l_t} + \frac{d_{.277}}{l_t}\left(nW - L_{t_{.277}}\right) + \frac{dd_{.277}}{dM} \frac{M}{l_t}\left(nW - L_{t_{.277}}\right) \tag{14}$$

For computing purposes, equation (14) was used as

$$L_{t_{.277}} = A \frac{q}{\sqrt{1 - M^2}} + B\left(nW - L_{t_{.277}}\right) + CM\left(nW - L_{t_{.277}}\right) \tag{15}$$

Seventy-six equations (two from each run) in the form of equation (15) were written, the low and high load-factor tail loads being used for each of the 38 runs. A standard least-squares normalizing process was used to reduce the equations for the determination of the coefficients A, B, and C. The use of the end points for each run automatically weighted the data so that the runs which covered a greater range of load factor and would be expected to produce the most reliable data were permitted to have a greater influence in the determination of the coefficients A, B, and C.

The coefficients A, B, and C of equation (15) and their standard errors were determined from the least-squares solution as

$$A = -22.45 \pm 0.62$$

$$B = 0.06366 \pm 0.00415$$

$$C = -0.02087 \pm 0.00839$$

The standard error of estimate s is ±552 pounds. Plotted in figure 7 are the tail loads calculated by the use of equation (15) and the values given previously for A, B, and C against the tail loads calculated by equations (13) for the same 76 points. The departures from the 45° correlation line and the s of ±552 pounds indicate rather poor correlation.

A clue to the reason for the poor correlation was found in ground deflection tests which indicated that as the temperature measured on the aft end of the fuselage decreased, the aft end of the fuselage deflected down at a rate of 1 in./100° F. The attachment of the horizontal tail to the fuselage causes a longitudinal restraint to the

bending due to temperature changes, which could introduce stresses in the horizontal tail influencing the strain gages in a manner similar to a carryover effect. In flight such an effect would produce an increment in measured tail load proportional to the change ΔT in fuselage structural temperature from ground to flight, since the ground position of each strain-gage trace was used as a reference in data evaluation, equation (2). In any one maneuver the change in ΔT was negligible; therefore, ΔT was introduced in an equation of the form of equation (15) as a term associated with the tail load as

$$L_{t.277} = A\frac{q}{\sqrt{1 - M^2}} + B\left(nW - L_{t.277}\right) + CM\left(nW - L_{t.277}\right) + D\Delta T \qquad (16)$$

The values of ΔT as used are listed in column (13) of table III(a).

From the least-squares solution of equation (16) the coefficients A, B, C, and D and their standard errors were now determined as

$$A = -22.40 \pm 0.25$$

$$B = 0.05614 \pm 0.00170$$

$$C = -0.01831 \pm 0.00336$$

$$D = 12.25 \pm 0.62$$

The standard error of estimate for the solution with the inclusion of the ΔT term is ± 221 pounds. A correlation plot for this solution similar to figure 7 is shown as figure 8. Comparison of figure 8 with figure 7 indicates a marked improvement in the correlation. The reduction of s from ± 552 pounds to ± 221 pounds is also statistically significant.

With the temperature correction factor established from coefficient D of equation (16) as 12 lb/°F, a temperature correction to the zero-lift pitching-moment coefficient $\Delta C_{m_{O_{\Delta T}}}$ was determined for all of the data for configuration A in the lower C_{N_A} range. The temperatures and corrections are listed in table III(a) along with the final computed C_{m_O} which is defined as

$$C_{m_O} = C_{m_{O_c}} - \Delta C_{m_{O_{\Delta T}}} \qquad (17)$$

A plot of C_{m_O} against M is shown in figure 9. The solid faired line through the data represents the curve defined by the coefficient A of equation (16) and its associated Mach number factor $1/\sqrt{1 - M^2}$.

Above a Mach number of 0.72, the curve is dashed to indicate that it is faired without the use of an equation. An abrupt increase in the absolute value of C_{m_0} occurs after $M = 0.72$ is reached with a maximum negative value being obtained at $M = 0.76$, near which Mach number the maximum down tail load at zero lift would be encountered. Illustrative of the accuracy in this Mach number range, the data points shown in figure 9 at $M = 0.76$ have estimated accuracies of ± 0.005 for 30,000 feet and ± 0.003 for 22,500 feet.

Aerodynamic-center position for the lower C_{N_A} range data is plotted in figure 10 as a function of Mach number. The use of the parameters B and CM from the least-squares fitting of equation (16) to the data gives the solid line shown in figure 10 from $M = 0.32$ to $M = 0.72$. The dashed line above $M = 0.72$ indicates fairing without the use of an equation. Above $M = 0.72$ the aerodynamic center moves rapidly forward and reaches approximately 7 percent $\bar{c}$ at $M = 0.77$.

Upper C_{N_A} range.- The method for correlating the upper C_{N_A} range data was similar to that used for the lower C_{N_A} range data as previously described. However, the small range of ΔT covered by the available data for the upper C_{N_A} range made it impractical to attempt the inclusion of ΔT as a correlating coefficient. The Glauert factor did not adequately represent the variation of C_{m_0} with Mach number; therefore, an acceptable form of the least-squares equation for this range of data was determined empirically to be

$$L_{t.277} - D\Delta T = E\frac{q}{M^3/2} + F\left(nW - L_{t.277}\right) + GM\left(nW - L_{t.277}\right) \qquad (18)$$

For the correction $D\Delta T$ to $L'_{t.277}$, the value of D used was determined from the data for configuration A in the lower C_{N_A} range. Values of $L'_{t.277}$ were calculated from equation (13), the values of x_{ac} and $C_{m_{0_c}}$ listed in table III(b) being used for the 24 runs available with Mach numbers to 0.72.

The coefficients E, F, and G determined from the least-squares solution of equation (18) were

$$E = -21.25 \pm 0.50$$

$$F = 0.1937 \pm 0.0034$$

$$G = -0.1951 \pm 0.0040$$

The standard error of estimate for this solution was ±234 pounds which compares favorably with the s of ±221 pounds from the solution for the lower C_{N_A} range.

The coefficients E, F, and G have no particular aerodynamic significance since values of C_{m_O} obtained from the coefficient E are merely extrapolations from a high lift range and not strictly speaking zero-lift wing-fuselage pitching-moment coefficients. They are useful for the calculation of horizontal-tail loads at conditions other than those tested.

A plot of C_{m_O} against M for the upper C_{N_A} range is shown in figure 11. Values of C_{m_O} are listed in column (15) of table III(b) as computed from equation (17). The solid faired line through the data represents the curve defined by the coefficient E of equation (18) and its empirically chosen Mach number variation $\frac{1}{M^{3/2}}$. The dashed-line curve above M = 0.72 indicates fairing without the use of an equation. In figure 11 the two data points shown as solid symbols at Mach numbers of 0.43 and 0.78 have estimated accuracies of ±0.0839 and ±0.0526, respectively.

Aerodynamic-center position for the upper C_{N_A} range data, tabulated in column (7) of table III(b), is plotted in figure 12 as a function of Mach number. The solid line represents the curve defined by the parameters F and GM of equation (18). The dashed line above M = 0.72 again indicates fairing without the use of an equation.

Analysis for Configuration B

Lower C_{N_A} range.- The form of the equation used to eliminate the temperature effect from the tail load measurements for configuration B was the same as that used for configuration A. The value of $C_{m_{O_c}}$ was assumed to vary with Mach number to M = 0.70 according to the Glauert factor, and the aerodynamic-center position was assumed to vary linearly to this same Mach number. Tail loads were computed by equations (13) for an average center-of-gravity value of 27.7 percent $\bar{c}$ from the $C_{m_{O_c}}$ and x_{ac} data given in table IV(a) for the highest and lowest load factor n for each run and used in the expression

$$L_{t.27} = A' \frac{q}{\sqrt{1 - M^2}} + B'\left(nW - L_{t.27}\right) + C'M\left(nW - L_{t.27}\right) + D'\Delta T \qquad (19)$$

to set up 74 equations for least-squares solution.

Equation (19) was also solved without the inclusion of the temperature term and the results of the two solutions may be compared in the following table, which also includes similar solutions for configuration A.

Configuration	Case	Coefficient				
		A or A'	B or B'	C or C'	D or D'	s, lb
A	I	-22.45 ± 0.62	0.06366 ± 0.00415	-0.02087 ± 0.00853	----------	±552
	II	-22.40 ± 0.25	0.05614 ± 0.00170	-0.01831 ± 0.00336	12.25 ± 0.62	±221
B	III	-8.81 ± 0.53	0.06047 ± 0.00338	-0.03022 ± 0.00695	----------	±506
	IV	-9.44 ± 0.22	0.04588 ± 0.00158	-0.01178 ± 0.00302	12.31 ± 0.65	±210

The most interesting feature of this table is the close agreement shown between the temperature coefficients of cases II and IV which are for two different airplane configurations. The coefficients A and A' for cases II and IV are markedly different because of the effect of change in configuration on the wing-fuselage zero-lift pitching-moment coefficient. The differences between the aerodynamic-center parameters B and B' and C and C' are less pronounced.

With the temperature correction factor established from coefficient D' of equation (19) as 12 lb/°F a value of $\Delta C_{m_{O_{\Delta T}}}$ was determined for all of the data for configuration B in the lower C_{N_A} range. The temperatures and corrections are listed in table IV(a) along with the final computed C_{m_O}, which is plotted in figure 13 as a function of Mach number. The solid faired curve through the data is derived from the coefficient A' of equation (19) and the associated factor $1/\sqrt{1 - M^2}$. Above a Mach number of 0.70 the curve is dashed to indicate a fairing without the use of an equation.

The aerodynamic-center position determined from the parameters B' and C'M of equation (19) is shown as the solid curve in figure 14, which also contains the x_{ac} data of table IV(a). Again, the dashed-line curve above $M = 0.70$ indicates fairing without the use of an equation. After reaching a maximum value of 20 percent $\bar{c}$ at $M = 0.74$, the aerodynamic center for configuration B moves forward to 12 percent $\bar{c}$ at $M = 0.775$.

Upper C_{N_A} range.- The empirical equation used to fit the tail loads calculated for a center of gravity at 27.7 percent $\bar{c}$ for Mach numbers up to 0.65 was

$$L_{t_{.277}} - D'\Delta T = E'\frac{q}{M^2} + F'\left(nW - L_{t_{.277}}\right) + G'M\left(nW - L_{t_{.277}}\right) \qquad (20)$$

For the correction $D'\Delta T$ to $L_{t_{.277}}$, the value of D' determined for the data for configuration B in the lower C_{N_A} range was used. Values of $L_{t_{.277}}$ were calculated from equations (13) by use of the values of x_{ac} and $C_{m_{O_c}}$ listed in table IV(b) for the 12 runs available with Mach numbers up to 0.65.

The coefficients E', F', and G' determined from the least-squares solution of equation (20) were

$$E' = -9.15 \pm 0.39$$

$$F' = 0.1570 \pm 0.0047$$

$$G' = -0.1586 \pm 0.0058$$

The data were fitted with a standard error of ± 129 pounds. The values of C_{m_O} and x_{ac} are listed in table IV(b) and are plotted in figures 15 and 16. The derived variations of C_{m_O} and x_{ac} with Mach number are also shown in figures 15 and 16 as the solid-line curves. Above $M = 0.65$ the curves are dashed to indicate an estimate of their shapes in this Mach number range.

ABRUPT PITCHING MANEUVERS

The abrupt pitching maneuvers made during the flight tests are listed in table II. Thirteen abrupt maneuvers were made during tests of configuration A and eighteen maneuvers during tests of configuration B. The maneuvers were made at a pressure altitude of approximately 20,000 feet; and generally those at the lower speeds were made as push-downs to -1.0g followed by pull-ups to 3.0g, whereas those at the higher speeds were made as pull-ups followed by push-downs. Maximum pitching accelerations reached were of the order of ± 1.3 radians/sec^2.

The presence of pitching acceleration requires an additional term in the equation for tail load. For a rigid airplane, equation (5) can be modified as

$$L_t = \frac{-C_{m_0} q S \bar{c}}{x_t} + \frac{nWd}{x_t} + \frac{I_y}{x_t} \ddot{\theta}_{cg} \tag{21}$$

For analysis of the tail loads measured in a given maneuver, equation (21) can be written as

$$L_{t_M} = L_{t_0} + \frac{dL_t}{dn} n + \frac{dL_t}{d\ddot{\theta}_{cg}} \ddot{\theta}_{cg} \tag{22}$$

Configuration A

Use of equation (22) in a least-squares analysis of the tail loads for the abrupt maneuvers listed in table II(a) indicated that this equation did not adequately represent the tail loads resulting from the airplane motion. For example, shown in figures 17 and 18 are time histories of measured quantities in typical abrupt maneuvers of configuration A for Mach numbers of 0.39 and 0.71. The Mach number and altitude are constant for each run. The elevator angle shown is, in these cases, the deflection at the root of the right elevator. Shown as circles in the time histories of n, $\ddot{\theta}_{cg}$, and L_{t_M} are the data which were used in the least-squares analysis of these maneuvers. The error of fit for equation (22) $\epsilon_{\ddot{\theta}_{cg}}$ is defined as

$$\epsilon_{\ddot{\theta}_{cg}} = L_{t_M} - (\text{Tail load calculated with coefficients of eq. (22)}) \tag{23}$$

The standard errors of estimate s of ±682 pounds and ±785 pounds are large compared to the measuring errors, and the maximum errors occur when the elevator has been displaced abruptly but before the airplane pitching acceleration as measured at the center of gravity has changed appreciably. This association of large errors with small values of pitching acceleration suggests the presence of an additional degree of freedom which is not accounted for by equations (21) or (22).

In an attempt to include some measure of fuselage flexibility effects in the tail-load equation, a measure of pitching acceleration $\ddot{\theta}_t$ shown in figures 17 and 18 was used. This measure is the angular acceleration obtained from the difference between the linear acceleration at the tail and that at the center of gravity and is defined by the equation

$$\ddot{\theta}_t = -\frac{g}{l_t}(n - n_t) \tag{24}$$

The time-history data of $\ddot{\theta}_t$ shown in figures 17 and 18 were used in a least-squares relationship of the type

$$L_{t_M} = L_{t_0} + \frac{dL_t}{dn} n + \frac{dL_t}{d\ddot{\theta}_t} \ddot{\theta}_t \tag{25}$$

The errors of fit for equation (25) defined by the equation

$$\epsilon_{\ddot{\theta}_t} = L_{t_M} - \left(\text{Tail load calculated with coefficients of eq. (25)} \right) \tag{26}$$

are shown in figures 17 and 18 for the two sample maneuvers. The standard errors of estimate reduced from over ±600 pounds to less than ±300 pounds for all abrupt maneuvers for configuration A. It is believed, therefore, that the zero-lift pitching-moment coefficient, aerodynamic-center position, and airplane pitching moment of inertia were determinable from the coefficients of equation (25) despite the presence of the additional degree of freedom. It was concluded that from the available instrumentation (NACA pitching accelerometer mounted near the center of gravity and linear accelerometers mounted near the center of gravity and in the tail) the parameters of this additional degree of freedom could not be established.

The corrected values of C_{m_0}, x_{ac}, and I_y derived by fitting the abrupt-maneuver data for configuration A obtained by least-squares solutions of equations of the form of equation (25) are listed in table V with identifying Mach numbers and run numbers. Also listed in table V are values of the radius of gyration k_y computed from I_y and the airplane weight for each run. Airplane weight, center of gravity, and mass distribution varied only slightly during all the maneuvers listed in table V and the k_y values indicate scatter from an average value by only ±0.5 foot.

The zero-lift pitching-moment coefficients listed in table V are corrected for temperature effects and plotted as a function of Mach number in figure 19 with the final C_{m_0} curves from figure 9 for the gradual maneuvers. The agreement is considered to be good.

The corrected x_{ac} values listed in table V are plotted as a function of Mach number in figure 20. The final aerodynamic-center-position curves determined for configuration A in gradual maneuvers (from fig. 10) are also shown. Again the agreement is considered to be good.

Configuration B

For the abrupt-pitching-maneuver tests with configuration B, the instrumentation was modified to include a linear accelerometer in the nose of the airplane. This addition and the assumption that the forward portion of the fuselage acted essentially as a rigid beam permitted the determination of pitching accelerations at the airplane center of gravity with less lag than when an angular accelerometer was used.

In figure 21 time histories of n, incremental tail acceleration Δa_t, pitching accelerations, elevator angle δ_e and L_{t_M} are shown for an abrupt push-pull maneuver at $M = 0.44$ at 20,000 feet pressure altitude. The three pitching-acceleration quantities shown are $\ddot{\theta}_{cg}$, $\ddot{\theta}_t$, and $\ddot{\theta}_r$. As before, the pitching acceleration $\ddot{\theta}_{cg}$ is from a direct measurement of the angular acceleration near the center of gravity and $\ddot{\theta}_t$ is defined by equation (24). The equation which defines $\ddot{\theta}_r$, the pitching acceleration of the assumed rigid portion of the airplane, is

$$\ddot{\theta}_r = \frac{g}{l_n}(n_n - n) \tag{27}$$

For analysis of the tail loads in abrupt maneuvers an incremental tail acceleration Δa_t is defined as the normal acceleration at the tail due to the difference between the angular acceleration of the tail and the angular acceleration of the (assumed) rigid forward portion of the airplane as

$$\Delta a_t = g\left[(n_t - n) - \frac{l_t}{l_n}(n_n - n)\right] = l_t(\ddot{\theta}_t - \ddot{\theta}_r) \tag{28}$$

In figure 21 it will be noted that the calculated $\ddot{\theta}_r$ values have a different time history during abrupt elevator displacements than either the $\ddot{\theta}_{cg}$ measurements or the calculated $\ddot{\theta}_t$ values. Although only the points used in least-squares calculations are shown, the time history of incremental tail acceleration Δa_t when evaluated in more detail than shown indicated an oscillation of the tail at the fuselage first bending frequency (8.0 cps).

Time histories are given in figure 22 of elevator angle, pitching acceleration $\ddot{\theta}_r$, incremental tail acceleration Δa_t, center-of-gravity load factor n, and L_{t_M} for a push-pull maneuver at $M = 0.70$ at 20,000 feet pressure altitude. The time history of incremental tail acceleration again shows peak values occurring during abrupt elevator displacements. In some runs the incremental tail acceleration exceeded 32.2 ft/sec^2. A rapid bending of the aft portion of the fuselage due

to abruptly applied elevator loads produces a damped free oscillation. The motion of the airplane is apparently coupled with this motion in such a manner than an additional term is required in the pitching-moment equation to evaluate the tail-load parameters as

$$L_t = -C_{m_0} \frac{qS\bar{c}}{x_t} + \frac{nWd}{x_t} + I_y \frac{\ddot{\theta}_r}{x_t} + M_e l_e \frac{\Delta a_t}{x_t} \tag{29}$$

The product $M_e l_e$ in equation (29) can be considered as the effective mass moment of the flexible fuselage acting as a single-degree-of-freedom cantilever beam. If the distance l_e is assumed to be the location of the tail accelerometer, the M_e term becomes the effective mass oscillating at this distance from the airplane center of gravity.

A comparison was made between various methods of analyzing the tail-loads data of the maneuver shown in figure 21. The methods involve least-squares solutions using each of the following equations based on available measures of the pitching accelerations and, in the case of equation (31), the inclusion of an additional degree of freedom:

Method I (equation (22))

$$L_{t_M} = L_{T_0} + \frac{dL_t}{dn} n + \frac{dL_t}{d\ddot{\theta}_{cg}} \ddot{\theta}_{cg}$$

Method II (equation (25))

$$L_{t_M} = L_{T_0} + \frac{dL_t}{dn} n + \frac{dL_t}{d\ddot{\theta}_t} \ddot{\theta}_t$$

Method III

$$L_{t_M} = L_{t_0} + \frac{dL_t}{dn} n + \frac{dL_t}{d\ddot{\theta}_r} \ddot{\theta}_r \tag{30}$$

Method IV

$$L_{t_M} = L_{t_0} + \frac{dL_t}{dn} n + \frac{dL_t}{d\ddot{\theta}_r} \ddot{\theta}_r + \frac{dL_t}{d\Delta a_t} \Delta a_t \tag{31}$$

The results of this analysis are shown graphically in figure 21 where time histories of the measured tail load and the errors of fit associated

with each method are presented. The following table lists the coefficients determined for each method and the standard errors of estimate:

Method	Coefficient						
	L_{t_0}	$\frac{dL_t}{dn}$	$\frac{dL_t}{d\ddot{\theta}_{cg}}$	$\frac{dL_t}{d\ddot{\theta}_t}$	$\frac{dL_t}{d\ddot{\theta}_r}$	$\frac{dL_t}{d\Delta a_t}$	s
I	-1,020	3,080	-4,990	------	------	---	±610
II	-590	2,040	------	-6,480	------	---	±230
III	-1,040	2,350	------	------	-5,350	---	±501
IV	-690	2,080	------	------	-6,320	155	±156

The poorest fit to the data is obtained by method I where an angular accelerometer at the center of gravity suspected of introducing errors due to its frequency response characteristics was used for $\ddot{\theta}_{cg}$. A comparison of the results for method I with the results for method III indicates a substantial improvement by using $\ddot{\theta}_r$. When method II is used, the standard error of estimate s drops to ±230 pounds indicating an improvement over both cases I and III. Use of method IV produced a significant change in the fit to the data but the primary coefficients L_{t_0}, $\frac{dL_t}{dn}$, and $\frac{dL_t}{d\ddot{\theta}}$ are essentially the same as those for method II. The results for the abrupt maneuver at M = 0.70 are shown in figure 22 with errors in fit for methods III and IV.

The results of analyses of all abrupt maneuvers for configuration B indicated that method IV was significantly better in each case.

The zero-lift pitching-moment coefficient derived from the L_{t_0} term of equation (31) was corrected for area, thrust, elevator angle, and temperature. The aerodynamic-center position x_{ac}, pitching moment of inertia I_y, and effective mass M_e were computed from pertinent coefficients in equation (31) and corrected for area and elevator angle. The results of these corrections for all runs are listed in table VI along with identifying run number and Mach number.

Zero-lift pitching-moment coefficients are plotted in figure 23 for the lower C_{N_A} range. The points shown as circles are values where corrections were made to the data for area, thrust, and elevator angle but not for temperature. When the temperature corrections are applied by using the

coefficient $\frac{dL_t}{d\Delta T} = 12.3$ lb/°F, the points shown as squares are obtained and are seen to be in excellent agreement with the faired gradual-turn data from figure 13.

The aerodynamic-center position is plotted in figure 24 and compared with the faired curves shown for the gradual-maneuver data in figure 14. The agreement is considered to be reasonably good.

The radius of gyration k_y listed in table VI was determined from the derived I_y values and the airplane weight and agrees with estimates based on manufacturer's data. There is an apparent trend toward increasing k_y as the runs are made from 18-1 to 18-18. The fuel is carried near the airplane center of gravity and consumption of fuel would tend to increase the radius of gyration.

The final tail-load parameter to be considered here is the effective mass M_e of the aft-fuselage-tail combination. The values tabulated in table VI range from a minimum value of 172 slugs for run 18-15 to a maximum value of 218 slugs for run 18-12, with an average value of 193 slugs. An effective mass parameter can be computed for the airplane using the equation

$$M_e = \frac{W_{tf} l_m}{l_e g} \tag{32}$$

where W_{tf} is the weight of the tail assembly and the fuselage rearward of the wing rear spar and l_m is the distance between the airplane center of gravity and the center of gravity of the weight W_{tf}. Numerically, equation (32) becomes

$$M_e = \frac{6130 \text{ lb} \times 339 \text{ in.}}{395 \text{ in.} \times 32.2 \text{ ft/sec}^2} = 163 \text{ slugs}$$

a value not too far removed from the average value of 193 slugs determined from the flight-test data.

COMPARISON WITH WIND-TUNNEL DATA

Wind-tunnel data relating to the longitudinal stability and control characteristics of an XB-45 airplane is contained in reference 2. The XB-45 is similar to configuration A of the present paper. The difference between the two airplanes is in the horizontal tail, which has little bearing on the comparison of tail-off pitching-moment data.

Wind-tunnel data were available at Mach numbers of 0.400, 0.600, 0.650, 0.675, 0.700, 0.725, 0.750, 0.775, 0.800, 0.825, and 0.850 for a configuration designated WBKN + D in reference 2. The configuration nomenclature refers to tests with wing, body, canopy, nacelles with dummy engines, and a dorsal fin installed. Tunnel test data were given in the form of pitching-moment coefficient about the center of gravity at $0.25\bar{c}$ plotted as a function of lift coefficient.

Comparisons between flight and wind-tunnel results are shown in figure 25 as plots of tail-off pitching-moment coefficient about the quarter chord $C_{m_{\bar{c}/4}}$ against wing-fuselage normal-force coefficient $C_{N_{wf}}$ for Mach numbers of 0.400, 0.600, 0.650, 0.700, 0.750, and 0.775. A Mach number of 0.775 represents the approximate upper limit of flight data for configuration A. The wind-tunnel data are shown as the points. The flight data are shown as solid lines and were obtained from the faired curves of C_{m_O} and x_{ac} shown in figures 9 to 12 by the use of the following equation:

$$C_{m_{\bar{c}/4}} = C_{m_O} - \frac{d}{\bar{c}} C_{N_{wf}} \tag{33}$$

At the two lowest Mach numbers good agreement is indicated between flight and wind-tunnel pitching-moment results in the lower lift range, but definite differences occur in the location of the aerodynamic centers. For example, the difference in the slopes of the flight and wind-tunnel data at $M = 0.600$ for the lower lift range amounts to an underestimation of the flight tail load of 600 pounds per g. More important, however, is the fact that the nonlinear variation of $C_{m_{\bar{c}/4}}$ with $C_{N_{wf}}$ shown for the flight data is also evident in the wind-tunnel data. It would seem that the calculation of design tail loads by analytical methods, which consider in detail the airplane motion using prescribed elevator-deflection time histories, is not warranted unless the analytical method can take into account such nonlinear pitching-moment characteristics as are exhibited in this case.

Reasonable agreement between flight and wind-tunnel data is also indicated for Mach numbers of 0.650 and 0.700, but the zero-lift pitching-moment coefficients for the wind-tunnel data are less negative than the flight values.

At the two highest Mach numbers rather serious departures may be noted between the flight and wind-tunnel data. For low lift coefficients at a Mach number of 0.750 the wind-tunnel data would give tail-load values which underestimate the flight values by approximately 8,500 pounds at 15,000 feet pressure altitude. At a Mach number of 0.775 the sudden increase in stability shown by the flight data above $C_{N_{wf}} = 0.2$ is not evident in the wind-tunnel data. Larger negative tail loads are indicated at high normal-force coefficients than at zero lift.

On the whole it can be stated that reasonable agreement is shown between wind-tunnel data and flight data for configuration A up to a Mach number of 0.700.

CALCULATION OF TAIL LOADS FOR CRITICAL FLIGHT CONDITIONS

In the following section some calculations of total horizontal-tail loads are given for configuration B based on flight data presented earlier. The type maneuver considered to produce the highest tail loads was one where a gradual or windup turn is made to the stall or limit load factor, from which point an abrupt recovery is made. Design center-of-gravity limits of 21 percent $\bar{c}$ and 32 percent $\bar{c}$ were used in the calculations, but, since the loads at 32 percent $\bar{c}$ were always greater, only this information is presented.

Gradual-Maneuver Tail Loads

The computed structural tail loads for balanced conditions L_{t_1} are shown in the upper portion of figure 26. The L_{t_1} loads defined by the following equation have not been corrected for tail pitching-moment increments due to elevator deflection or airplane pitching moments due to engine thrust.

$$L_{t_1} = -C_{m_O} q \frac{S\bar{c}}{x_t} + \frac{nWd}{x_t} - n_t W_t \tag{34}$$

The computed loads shown in figure 26 apply to the design gross weight of 82,600 pounds with a center-of-gravity location of 32 percent $\bar{c}$ for either the positive design load factor of 3.0g or the load factor associated with the stall.

Stall load factors were computed by use of the buffet or stall boundary which is shown in the lower half of figure 26 in terms of C_{N_A} and M. The airplane normal-force coefficient at which the break from lower to upper C_{N_A} range occurs is indicated by the curve labeled break boundary. This break boundary was obtained by solving the following simultaneous equations for $C_{N_{wf}}$ with the assumption that $C_{N_A} \approx C_{N_{wf}}$

$$\left.\begin{aligned} C_{m_{cg}} &= C_{m_{O_{lower}}} - \frac{d_{lower}}{\bar{c}} C_{N_{wf}} \\ C_{m_{cg}} &= C_{m_{O_{upper}}} - \frac{d_{upper}}{\bar{c}} C_{N_{wf}} \end{aligned}\right\} \tag{35}$$

The values of C_{m_0} and aerodynamic-center position used in equations (35) were obtained from the faired curves of figures 13 to 16.

The tail loads shown in figure 26 were computed for standard pressure altitudes of sea level, 15,000 feet, and 30,000 feet. On the sea-level curve, point Ⓐ is limited by stall as shown on the buffet-boundary curve and is below the break boundary. Data between points Ⓐ and Ⓑ are below the break boundary. From point Ⓑ to point Ⓒ the buffet boundary lies above the break boundary and tail loads were calculated by using the upper C_{N_A} range data. Point Ⓒ is the lowest Mach number at which 3.0g is reached at sea level on the stall or buffet boundary, and this 3.0g limit line is used for the calculations through points Ⓓ and Ⓔ and up to the maximum Mach number of the calculations. Between points Ⓓ and Ⓔ the airplane is operating again below the break boundary. On the sea-level curve the maximum up tail load occurs at $M = 0.42$ and is approximately 9,000 pounds. The maximum down tail load at sea level for a 3.0g maneuver is not critical.

Similar calculations shown for 15,000 feet indicate a maximum up tail load of 9,000 pounds at $M = 0.57$, whereas at 30,000 feet a 13,000-pound tail load is calculated at the maximum Mach number.

Information concerning the buffet boundary and break boundary at negative airplane normal-force coefficients was not obtained during the flight tests; therefore, the assumption was made for the data plotted in figure 27 that these boundaries are merely the negative images of the positive lift boundaries. The structural tail loads shown in the upper portion of figure 27 are again computed by equation (34) as limited by the assumed stall and break boundaries. The critical tail load is seen to occur at sea level at a Mach number of about 0.77. Since there was a limit design Mach number for the airplane which varied with altitude, a shaded region is shown which represents tail loads unattainable without exceeding the design limits. Points along the upper boundary of the shaded region represent the tail load at design Mach numbers varying from 0.715 at sea level to 0.775 at approximately 4,000 feet.

Buffeting Tail Loads

Figure 26 indicates that buffeting could be encountered without exceeding 3.0g under the following conditions: at sea level at Mach numbers to $M = 0.42$, at 15,000 feet at Mach numbers to 0.57, and at all Mach numbers at 30,000 feet. Buffeting loads data obtained during the flight tests at high altitudes were extrapolated to 15,000 feet and sea-level conditions on the basis that the maximum buffeting load at a given Mach number would vary with the square root of the dynamic pressure as indicated by the buffeting analyses reported in reference 3.

The assumption was made that the buffeting loads measured at 30,000 feet represented maximum loads from the standpoint of length of time in buffeting and penetration beyond the buffet boundary. In the upper part of figure 28 these calculated buffeting loads are shown as a function of altitude and Mach number. The shaded area represents loads unattainable without exceeding the 3.0g limit.

In the lower half of figure 28 the load

$$L_{t_2} = L_{t_1} + \Delta L_{t_B} \tag{36}$$

is shown for sea level, 15,000 feet, and 30,000 feet and for the 3.0g limit line. With the inclusion of buffeting loads it will be noted that the maximum up tail load now occurs in what would be the upper left-hand corner of a sea-level V-n diagram. The maximum structural tail load at this point is now 17,000 pounds.

No buffet load calculations are shown for negative load factors, since they do not produce critical loadings.

Maximum Structural Tail Loads

The maximum values of tail loads from figures 27 and 28 for both positive and negative load factors in gradual maneuvers are shown in figure 29 as the L_{t_2} curves. The small corrections in tail load necessary to balance the airplane with elevator deflected and with power on were estimated and added to the L_{t_2} curves to give the final structural tail load L_{t_3} for balanced flight at either stall or limit load factor. The maximum up tail load is now 18,000 pounds and the maximum down tail load is -27,000 pounds.

If a recovery from either the maximum up-tail-load condition or the maximum down tail-load condition is effected by an abrupt control displacement, the loads will be increased in each case by an amount equal to

$$\Delta L_{t_{\ddot{\theta}}} = \frac{I_y}{x_t} \ddot{\theta}_{cg} - \frac{l_t}{g} \ddot{\theta}_{cg} W_t \tag{37}$$

where the term $\frac{l_t}{g} \ddot{\theta}_{cg} W_t$ is the incremental inertia load due to pitching acceleration. With a radius of gyration of 12.5 feet, an airplane weight

of 82,600 pounds, and with the center of gravity at 32 percent $\bar{c}$, equation (37) becomes

$$\Delta L_{t_{\ddot{\theta}}} = 11{,}400\ddot{\theta}_{cg} - 1{,}100\ddot{\theta}_{cg}$$

$$= 10{,}300\ddot{\theta}_{cg}$$

Pitching-acceleration values as high as ± 1.3 radians/sec^2 have been measured with the test airplane in maneuvers made for the specific purpose of reaching maximum pitching accelerations. Thus, the pitching-acceleration tail load could equal $\pm 13{,}400$ pounds. Statistical data for other military aircraft indicate that values of pitching acceleration reached in military flying are usually well below airplane capabilities. The maximum increment in tail load due to the whipping of the aft portion of the fuselage (the $\frac{M_e l_e \Delta a_t}{x_t}$ term of equation (29)) was observed to be slightly out of phase with the maximum pitching-acceleration values in abrupt maneuvers. Although this term could contribute $\pm 4{,}000$ pounds to the tail load, it seems more reasonable to consider only 2,000 pounds as the addition to the critical tail load in the present simplified analysis.

Thus, the maximum up tail load would become the summation of 18,000 pounds (balancing structural load), 13,000 pounds (pitching-acceleration structural load), and 2,000 pounds (whipping structural load), or 33,000 pounds. According to information received from the airplane manufacturer, the limit up load for the stabilizer was 18,500 pounds and the stabilizer was tested to 150 percent of limit load, or 27,800 pounds without failure. Although the calculated 33,000-pound value applies to sea-level conditions, it can be seen from figure 28 that the balancing and buffeting loads are approximately at the sea-level value for all altitudes below 15,000 feet. The design limit up tail load can be exceeded at altitudes below 15,000 feet with only moderately abrupt recoveries from turns to high normal load factors.

The maximum structural down tail load from the present calculations is -42,000 pounds (-27,000 - 13,000 - 2,000). The manufacturer's limit down-tail load has been stated to be -24,100 pounds, and the tail has successfully withstood 157 percent limit load, or -37,800 pounds, without failure. Again the sea-level calculations used here are slightly extreme, but abrupt recoveries from negative design load-factor conditions at altitudes below 15,000 feet would produce structural tail loads in excess of the design limit values for Mach numbers above about 0.70.

CONCLUDING REMARKS

Horizontal-tail-loads data for two configurations of a multiengine jet bomber tested by the NACA have been summarized. For both configurations, analyses of the data indicated that temperature-introduced errors in strain-gage loads measurements may be compensated for in the data-analysis procedure, providing a sufficient variation in structural temperature is available to permit the inclusion of a temperature correction term in least-squares equations relating loads measurements to basic aerodynamic parameters.

An important effect of flexibility encountered during the tests on the airplane in longitudinal maneuvers was a whipping of the aft portion of the fuselage associated with abruptly applied tail loads. This flexibility effect necessitated the inclusion of an effective-mass (of the rearward part of the fuselage) term in the analysis of all abrupt pitching maneuvers to represent the airplane motion adequately.

The comparisons of aerodynamic parameters derived from gradual and abrupt maneuvers showed good agreement for both configurations.

Wind-tunnel tests appear to predict adequately the tail-off pitching-moment characteristics of the test airplane; at least up to Mach numbers of 0.700. The departures shown between wind-tunnel and flight data above $M = 0.700$ are serious.

It would appear from examination of wind-tunnel and flight pitching-moment data that involved computations for evaluating design tail loads are not warranted unless the nonlinearities in the aerodynamic data are considered.

For the test airplane excellent agreement was found between temperature correction coefficients for tail loads for both airplane configurations tested. The determinations of the airplane pitching-moment-of-inertia from flight data were consistent and in good agreement with estimates based on manufacturer's data. The effective mass of the tail-fuselage combination was in agreement with calculations based on static-weight-distribution considerations.

Horizontal-tail loads for the configuration of the test airplane (referred to as configuration B in the text) were shown to exceed design limit loads for low-speed low-altitude abrupt recoveries from stall

buffeting and for high-speed low-altutude abrupt recoveries from negative design load-factor maneuvers.

Langley Aeronautical Laboratory,
National Advisory Committee for Aeronautics,
Langley Field, Va., November 1, 1954.

REFERENCES

1. Skopinski, T. H., Aiken, William S., Jr., and Huston, Wilber B.: Calibration of Strain-Gage Installations in Aircraft Structures for the Measurement of Flight Loads. NACA TN 2993, 1953. (Supersedes NACA RM L52G31.)

2. Zebb, Keirn: Report on Wind-Tunnel Tests of a 1/10th-Scale Model of the XB-45 Airplane. Vol. I - Summary, Description, and Discussion of Tests; Build-up, Longitudinal Stability and Control Data. CWT Rep. 7, Southern Calif. Cooperative Wind Tunnel, Feb. 13, 1948.

3. Huston, Wilber B., and Skopinski, T. H.: Measurement and Analysis of Wing and Tail Buffeting Loads on a Fighter-Type Airplane. NACA TN 3080, 1954.

TABLE I.- AIRPLANE CHARACTERISTICS

Wing:	
Span, ft	89.04
Area, sq ft	1,175
Mean aerodynamic chord, ft	14.02
Airfoil, root	NACA 66,2-215
Airfoil, tip	NACA 66,1-212
Taper ratio	0.413
Horizontal tail surfaces:	
Area (including fuselage), sq ft	289.44
Span, ft	43.87
Elevator:	
Area (including tabs), sq ft	67.7

TABLE II.- SUMMARY OF FLIGHT TEST CONDITIONS

[M_{av} and q_{av} are average values for low lift-coefficient range]

(a) Configuration A

Type maneuver	Flight and run	Approximate test altitude, ft	M_{av}	q_{av}, lb/ft^2	W, lb	Center-of-gravity position, percent $\bar{c}$	Figure showing data
Gradual	4-2	30,000	0.38	63	61,600	28.3	-
Gradual	4-3	30,000	.43	81	60,900	28.3	-
Gradual	4-4	30,000	.48	101	59,900	28.2	3
Gradual	4-5	30,000	.53	122	59,100	28.1	-
Gradual	4-6	30,000	.59	148	58,100	28.0	-
Gradual	4-7	30,000	.64	178	57,400	27.9	-
Gradual	4-8	30,000	.70	210	56,600	27.8	-
Gradual	4-9	30,000	.72	233	56,300	27.8	3
Gradual	4-10	30,000	.74	252	55,800	27.7	-
Gradual	4-11	30,000	.77	279	55,200	27.6	-
Gradual	4-12	30,000	.78	286	54,400	27.6	-
Gradual	6-3	22,500	.42	106	62,700	28.2	-
Gradual	6-4	22,500	.47	137	62,400	28.1	3
Gradual	6-5	22,500	.52	161	61,600	28.1	-
Gradual	6-6	22,500	.58	203	60,500	27.9	-
Gradual	6-7	22,500	.63	241	59,700	27.8	-
Gradual	6-10	22,500	.76	360	58,000	27.6	-
Gradual	6-11	15,000	.37	117	56,400	27.5	-
Gradual	6-12,13	15,000	.32	83	56,000	27.4	-
Gradual	6-14	15,000	.42	148	55,600	27.4	-
Gradual	6-15	15,000	.47	183	55,300	27.3	3
Gradual	7-1	22,500	.36	83	63,600	28.2	-
Gradual	7-2	22,500	.45	124	62,900	28.1	-
Gradual	7-3	22,500	.56	199	62,100	28.1	-
Gradual	7-4	22,500	.62	238	61,300	28.0	-
Gradual	7-5	22,500	.67	273	60,200	27.8	-
Gradual	7-6	22,500	.70	305	59,600	27.8	-
Gradual	7-7	22,500	.72	328	58,300	27.6	3
Gradual	7-8	22,500	.75	348	57,800	27.6	-
Gradual	7-15	15,000	.51	213	56,000	27.4	-
Gradual	7-16	15,000	.54	238	55,700	27.4	-
Gradual	7-17	15,000	.57	262	55,400	27.3	-
Gradual	7-18	15,000	.60	303	55,100	27.3	-

TABLE II.- SUMMARY OF FLIGHT TEST CONDITIONS - Continued

[M_{av} and q_{av} are average values for low lift-coefficient range]

(a) Configuration A - Concluded

Type maneuver	Flight and run	Approximate test altitude, ft	M_{av}	q_{av}, lb/ft^2	W, lb	Center-of-gravity position, percent $\bar{c}$	Figure showing data
Gradual	7-19	15,000	0.63	332	54,800	27.2	--
Gradual	7-20	15,000	.65	361	54,200	27.2	--
Gradual	7-21	15,000	.68	395	53,800	27.1	--
Gradual	7-22	15,000	.71	408	53,200	27.1	--
Gradual	7-23	15,000	.73	457	52,900	27.1	3
Gradual	10-1	35,400	.60	123	61,800	27.7	--
Gradual	10-2	34,600	.65	149	61,500	27.7	--
Gradual	10-3	34,200	.67	160	61,200	27.6	--
Gradual	10-4	33,600	.70	182	60,800	27.6	--
Gradual	10-5	33,400	.73	199	60,300	27.5	--
Gradual	10-6	34,500	.68	166	59,900	27.5	--
Gradual	10-7	33,600	.72	194	59,500	27.4	--
Gradual	10-8	30,000	.77	261	59,200	27.4	--
Gradual	10-9	28,000	.76	271	58,800	27.3	--
Gradual	10-10	30,000	.74	246	58,300	27.2	--
Gradual	10-12	30,000	.56	139	56,900	27.1	--
Gradual	10-13	30,000	.53	124	56,700	27.0	--
Gradual	10-14	30,000	.48	103	56,500	27.0	--
Abrupt	8-2	20,000	.39	108	62,500	28.4	17
Abrupt	8-3	20,000	.45	136	61,700	28.4	--
Abrupt	8-4	20,000	.50	171	60,800	28.4	--
Abrupt	8-5	20,000	.55	208	60,100	28.3	--
Abrupt	8-6	20,000	.61	250	59,700	28.3	--
Abrupt	8-7	20,000	.66	298	58,800	28.4	--
Abrupt	8-8	20,000	.69	330	58,300	28.4	--
Abrupt	8-9	20,000	.71	350	57,900	28.6	18
Abrupt	8-10	20,000	.73	359	57,400	28.9	--
Abrupt	8-11	20,000	.75	390	57,000	29.1	--
Abrupt	8-12	20,000	.75	404	56,600	29.3	--
Abrupt	8-13	20,000	.66	298	55,800	29.5	--
Abrupt	8-14	20,000	.50	169	55,300	29.7	--

TABLE II.- SUMMARY OF FLIGHT TEST CONDITIONS - Continued

[M_{av} and q_{av} are average values for low lift-coefficient range]

(b) Configuration B

Type maneuver	Flight and run	Approximate test altitude, ft	M_{av}	q_{av}, lb/ft^2	W, lb	Center-of-gravity position, percent $\bar{c}$	Figure showing data
Gradual	11-1	30,000	[a]0.38	[a]66	63,500	28.1	-
Gradual	11-2	30,000	.42	78	62,900	28.0	-
Gradual	11-3	30,000	.45	91	62,500	28.0	-
Gradual	11-4	30,000	.48	102	62,100	27.9	5
Gradual	11-5	30,000	.51	115	61,600	27.9	-
Gradual	11-6	30,000	.55	129	60,900	27.8	-
Gradual	11-7	30,000	.58	150	60,400	27.7	-
Gradual	11-8	30,000	.61	161	59,900	27.7	-
Gradual	11-9	30,000	.65	185	59,300	27.6	-
Gradual	11-10	30,000	.68	204	59,100	27.6	-
Gradual	11-11	30,000	.70	211	58,500	27.5	-
Gradual	11-12	30,000	.72	223	58,100	27.4	5
Gradual	11-13	30,000	.74	243	57,700	27.4	-
Gradual	11-14	30,000	.76	263	57,300	27.3	-
Gradual	11-15	30,000	.78	284	56,700	27.2	-
Gradual	13-1	22,500	.35	78	62,800	28.1	-
Gradual	13-2	22,500	.36	81	62,500	28.1	-
Gradual	13-3	22,500	.38	87	62,200	28.0	-
Gradual	13-4	22,500	.40	98	61,900	28.0	-
Gradual	13-5	22,500	.44	119	61,700	28.0	-
Gradual	13-6	22,500	.48	143	61,100	27.9	5
Gradual	13-7	22,500	.53	171	60,500	27.8	-
Gradual	13-8	22,500	.57	200	59,900	27.7	-
Gradual	13-9	22,500	.62	235	59,400	27.7	-
Gradual	13-10	22,500	.66	269	58,400	27.6	-
Gradual	13-11	22,500	.68	285	57,900	27.5	-
Gradual	13-12	22,500	.70	295	57,200	27.4	-
Gradual	13-13	22,500	.72	316	56,700	27.4	5
Gradual	13-14	22,500	.74	340	55,900	27.3	-
Gradual	13-15	22,500	.75	359	55,500	27.2	-
Gradual	13-16	22,500	.77	393	55,100	27.2	-

[a]These two values are values for high-lift-coefficient range.

TABLE II.- SUMMARY OF FLIGHT TEST CONDITIONS - Concluded

[M_{av} and q_{av} are average values for low lift-coefficient range]

(b) Configuration B - Concluded

Type maneuver	Flight and run	Approximate test altitude, ft	M_{av}	q_{av}, lb/ft^2	W, lb	Center-of-gravity position, percent $\bar{c}$	Figure showing data
Gradual	15-1A	15,000	0.76	481	64,100	28.2	--
Gradual	15-1B	15,000	.76	502	64,100	28.2	--
Gradual	15-2	15,000	.74	454	61,300	27.9	--
Gradual	15-3	15,000	.71	433	60,700	27.8	5
Gradual	15-4	15,000	.70	413	59,900	27.8	--
Gradual	15-5	15,000	.68	390	59,500	27.7	--
Gradual	15-6	15,000	.66	358	59,200	27.7	--
Gradual	15-7	15,000	.64	346	58,900	27.6	--
Gradual	15-8	15,000	.62	318	58,600	27.6	--
Gradual	15-9	15,000	.60	300	58,400	27.6	--
Gradual	15-10	15,000	.57	277	58,200	27.5	--
Gradual	15-11	15,000	.53	238	58,000	27.5	--
Gradual	15-12	15,000	.49	202	57,900	27.5	5
Gradual	15-13	15,000	.45	167	57,600	27.4	--
Gradual	15-14	15,000	.40	134	57,500	27.4	--
Gradual	15-15	15,000	.38	123	57,300	27.4	--
Gradual	15-16	15,000	.36	111	57,200	27.4	--
Gradual	15-17	15,000	.35	100	57,000	27.3	--
Gradual	15-18	15,000	.40	137	56,700	27.3	--
Abrupt	18-1	20,000	.74	367	63,400	28.0	--
Abrupt	18-2	20,000	.72	359	62,300	27.9	--
Abrupt	18-3	20,000	.72	350	61,600	27.8	--
Abrupt	18-4	20,000	.70	338	61,000	27.7	--
Abrupt	18-5	20,000	.70	338	60,500	27.7	22
Abrupt	18-6	20,000	.67	307	60,200	27.6	--
Abrupt	18-7	20,000	.65	294	60,000	27.6	--
Abrupt	18-8	20,000	.62	262	59,600	27.6	--
Abrupt	18-9	20,000	.58	230	59,300	27.5	--
Abrupt	18-10	20,000	.54	197	59,100	27.5	--
Abrupt	18-11	20,000	.50	169	58,900	27.4	--
Abrupt	18-12	20,000	.44	134	58,800	27.4	21
Abrupt	18-13	20,000	.40	109	58,700	27.4	--
Abrupt	18-14	20,000	.35	82	58,600	27.4	--
Abrupt	18-15	20,000	.55	206	58,300	27.4	--
Abrupt	18-16	20,000	.50	169	58,200	27.3	--
Abrupt	18-17	20,000	.49	167	58,100	27.3	--
Abrupt	18-18	20,000	.45	134	58,000	27.3	--

TABLE III.- SUMMARY OF PITCHING-MOMENT CHARACTERISTICS

FOR CONFIGURATION A IN GRADUAL MANEUVERS

(a) Lower C_{N_A} range

(1)	(2)	(3)	(4)	(5)	(6)	(7)	(8)	(9)	(10)	(11)	(12)	(13)	(14)	(15)
Flight and run	Approximate altitude	Mach number	x_{ac_m}	$\Delta x_{ac_{area}}$	Δx_{ac_δ}	x_{ac}	$C_{m_{O_m}}$	$\Delta C_{m_{O_{area}}}$	$\Delta C_{m_{O_\delta}}$	$\Delta C_{m_{O_{thrust}}}$	$C_{m_{O_c}}$	ΔT, °F	$\Delta C_{m_{O_{\Delta T}}}$	C_{m_O}
6-12,13	15,000	0.32	15.4	-1.7	1.0	14.7	-0.0386	-0.0054	0.0031	0.0023	-0.0432	28	0.0087	-0.0519
6-11	15,000	.37	16.7	-1.5	1.0	16.2	-.0370	-.0052	.0030	.0019	-.0411	28	.0062	-.0473
6-14	15,000	.42	17.2	-1.4	.9	16.7	-.0382	-.0053	.0025	.0016	-.0428	27	.0047	-.0475
6-15	15,000	.47	16.7	-1.5	.9	16.1	-.0446	-.0062	.0022	.0015	-.0501	21	.0030	-.0531
7-15	15,000	.51	18.1	-1.3	.9	17.7	-.0410	-.0057	.0024	.0015	-.0458	21	.0025	-.0483
7-16	15,000	.54	17.4	-1.4	1.0	17.0	-.0441	-.0061	.0028	.0017	-.0491	18	.0020	-.0511
7-17	15,000	.57	17.6	-1.4	1.1	17.3	-.0456	-.0063	.0029	.0015	-.0505	15	.0015	-.0520
7-18	15,000	.60	18.2	-1.3	1.2	18.1	-.0462	-.0064	.0028	.0014	-.0512	10	.0008	-.0520
7-19	15,000	.63	17.5	-1.3	1.2	17.4	-.0501	-.0070	.0028	.0014	-.0557	8	.0006	-.0563
7-20	15,000	.65	17.5	-1.3	1.3	17.5	-.0524	-.0073	.0027	.0013	-.0583	5	.0004	-.0587
7-21	15,000	.68	18.5	-1.2	1.4	18.7	-.0526	-.0073	.0026	.0013	-.0586	4	.0003	-.0589
7-22	15,000	.71	17.1	-1.4	1.6	17.3	-.0590	-.0082	.0027	.0013	-.0658	4	.0003	-.0661
7-23	15,000	.73	15.8	-1.6	1.7	15.9	-.0659	-.0092	.0022	.0012	-.0741	1	.0001	-.0742
7-1	22,500	.36	16.3	-1.7	.8	15.4	-.0360	-.0050	.0028	.0029	-.0411	49	.0153	-.0564
6-3	22,500	.42	15.7	-1.7	.9	14.9	-.0420	-.0058	.0034	.0023	-.0467	53	.0130	-.0597
7-2	22,500	.45	16.9	-1.6	.9	16.2	-.0408	-.0057	.0029	.0020	-.0456	49	.0102	-.0558
6-4	22,500	.47	16.7	-1.6	.8	1_.9	-.0419	-.0058	.0029	.0018	-.0466	51	.0096	-.0562
6-5	22,500	.52	16.1	-1.7	.9	15.3	-.0447	-.0062	.0028	.0018	-.0499	51	.0082	-.0581
7-3	22,500	.56	17.7	-1.4	.9	17.2	-.0452	-.0063	.0026	.0014	-.0503	44	.0057	-.0560
6-6	22,500	.58	16.6	-1.6	1.0	16.0	-.0458	-.0064	.0029	.0016	-.0509	48	.0061	-.0570
7-4	22,500	.62	18.3	-1.4	1.0	17.9	-.0467	-.0065	.0029	.0013	-.0516	38	.0041	-.0557
6-7	22,500	.63	18.0	-1.4	1.0	17.6	-.0452	-.0063	.0028	.0014	-.0501	45	.0048	-.0549
7-5	22,500	.67	17.6	-1.4	1.0	17.2	-.0524	-.0073	.0029	.0014	-.0582	36	.0034	-.0616
7-6	22,500	.70	18.2	-1.3	1.2	18.1	-.0539	-.0075	.0030	.0013	-.0597	34	.0029	-.0628
7-7	22,500	.72	16.8	-1.5	1.3	16.6	-.0617	-.0086	.0029	.0013	-.0687	34	.0027	-.0714
7-8	22,500	.75	13.9	-1.9	1.6	13.6	-.0704	-.0098	.0025	.0013	-.0790	32	.0024	-.0814
6-10	22,500	.76	11.1	-2.3	1.7	10.5	-.0732	-.0102	.0023	.0012	-.0823	37	.0027	-.0850
4-3	30,000	.43	14.2	-2.0	.9	13.1	-.0435	-.0060	.0029	.0021	-.0487	94	.0302	-.0789
4-4	30,000	.48	15.6	-1.7	.7	14.6	-.0380	-.0053	.0016	.0021	-.0438	95	.0244	-.0782
10-14	30,000	.48	16.6	-1.4	.9	16.1	-.0298	-.0041	.0031	.0024	-.0332	79	.0199	-.0531
10-13	30,000	.53	16.2	-1.5	1.0	15:7	-.0359	-.0050	.0032	.0020	-.0397	77	.0161	-.0558
4-5	30,000	.53	16.4	-1.6	.9	15.7	-.0366	-.0051	.0023	.0019	-.0413	95	.0202	-.0615
10-12	30,000	.56	15.4	-1.6	.9	14.7	-.0422	-.0059	.0032	.0017	-.0466	77	.0144	-.0610
4-6	30,000	.59	16.1	-1.6	.9	15.4	-.0435	-.0060	.0026	.0018	-.0487	92	.0161	-.0648
4-7	30,000	.64	15.6	-1.7	.9	14.8	-.0505	-.0070	.0024	.0016	-.0567	90	.0132	-.0699
4-8	30,000	.70	17.9	-1.4	.9	17.4	-.0481	-.0067	.0023	.0012	-.0537	84	.0103	-.0640
4-9	30,000	.72	17.5	-1.4	.9	17.0	-.0545	-.0076	.0019	.0013	-.0615	86	.0095	-.0710
4-10	30,000	.74	15.4	-1.7	1.0	14.7	-.0654	-.0091	.0015	.0012	-.0742	84	.0087	-.0829
10-10	30,000	.74	16.7	-1.5	1.3	16.5	-.0600	-.0083	.0033	.0014	-.0664	72	.0076	-.0740
10-9	30,000	.76	9.1	-2.5	1.1	7.7	-.0710	-.0099	.0020	.0013	-.0802	73	.0072	-.0874
4-11	30,000	.77	14.8	-1.5	1.1	14.4	-.0564	-.0078	.0005	.0011	-.0648	92	.0086	-.0734
10-8	30,000	.77	8.0	-2.7	1.4	6.7	-.0656	-.0091	.0017	.0013	-.0743	75	.0077	-.0820
4-12	30,000	.78	11.2	-2.3	.7	9.6	-.0465	-.0065	-.0014	.0011	-.0555	97	.0090	-.0645
10-1	35,400	.60	14.6	-1.8	1.0	13.8	-.0460	-.0064	.0038	.0022	-.0508	85	.0179	-.0687
10-3	34,200	.67	16.3	-1.6	1.0	15.7	-.0472	-.0066	.0033	.0018	-.0523	83	.0134	-.0657
10-6	34,500	.68	16.4	-1.5	.9	15.8	-.0493	-.0069	.0033	.0017	-.0546	82	.0128	-.0674
10-4	33,600	.70	16.1	-1.6	.9	15.4	-.0507	-.0070	.0030	.0016	-.0563	82	.0118	-.0681
10-7	33,600	.72	17.1	-1.4	1.1	16.8	-.0488	-.0068	.0036	.0015	-.0535	79	.0105	-.0640
10-5	33,400	.73	18.3	-1.3	1.0	18.0	-.0487	-.0068	.0030	.0015	-.0540	79	.0102	-.0642

TABLE III.- SUMMARY OF PITCHING-MOMENT CHARACTERISTICS

FOR CONFIGURATION A IN GRADUAL MANEUVERS - Concluded

(b) Upper C_{N_A} range

(1)	(2)	(3)	(4)	(5)	(6)	(7)	(8)	(9)	(10)	(11)	(12)	(13)	(14)	(15)
Flight and run	Approximate altitude	Mach number	x_{ac_m}	$\Delta x_{ac_{area}}$	Δx_{ac_δ}	x_{ac}	$C_{m_{O_m}}$	$\Delta C_{m_{O_{area}}}$	$\Delta C_{m_{O_\delta}}$	$\Delta C_{m_{O_{thrust}}}$	$C_{m_{O_c}}$	ΔT, °F	$\Delta C_{m_{O_{\Delta T}}}$	C_{m_O}
6-4	22,500	0.48	11.0	-2.4	1.0	9.6	-0.0761	-0.0106	0.0037	0.0018	-0.0848	51	0.0096	-0.0944
6-5	22,500	.53	8.3	-2.7	1.1	6.7	-.0885	-.0123	.0036	.0018	-.0990	51	.0082	-.1072
7-3	22,500	.57	9.4	-2.6	1.2	8.0	-.0879	-.0122	.0042	.0014	-.0973	44	.0057	-.0930
6-6	22,500	.58	11.1	-2.3	1.0	9.8	-.0724	-.0101	.0027	.0016	-.0814	48	.0061	-.0875
7-4	22,500	.62	12.4	-2.2	1.2	11.4	-.0715	-.0099	.0038	.0013	-.0789	38	.0041	-.0830
6-7	22,500	.64	14.5	-1.9	.9	13.5	-.0587	-.0082	.0022	.0014	-.0661	45	.0048	-.0709
7-5	22,500	.68	14.4	-1.9	.9	13.4	-.0644	-.0090	.0023	.0014	-.0725	36	.0034	-.0759
10-1	35,400	.60	11.4	-2.3	.9	10.0	-.0612	-.0085	.0028	.0022	-.0691	85	.0179	-.0870
10-2	34,600	.65	14.3	-1.9	.6	13.0	-.0523	-.0073	.0011	.0019	-.0604	85	.0149	-.0753
10-3	34,200	.67	13.5	-2.0	.7	12.2	-.0596	-.0083	.0020	.0018	-.0677	85	.0134	-.0811
10-6	34,500	.68	13.6	-1.9	.7	12.4	-.0612	-.0085	.0021	.0017	-.0693	82	.0128	-.0821
10-4	33,600	.70	15.3	-1.7	1.0	14.6	-.0541	-.0075	.0035	.0016	-.0597	82	.0118	-.0715
10-7	33,600	.72	14.6	-1.8	1.1	13.9	-.0593	-.0082	.0040	.0015	-.0650	79	.0105	-.0755
10-5	33,400	.73	14.9	-1.8	1.1	14.2	-.0620	-.0086	.0034	.0015	-.0687	79	.0102	-.0789
4-2	30,000	.38	2.3	-3.6	1.9	.6	-.1306	-.0182	.0120	.0034	-.1402	91	.0394	-.1796
4-3	30,000	.43	-6.9	-4.9	2.5	-9.3	-.2065	-.0287	.0156	.0021	-.2217	94	.0302	-.2519
4-4	30,000	.48	5.7	-3.1	1.5	4.1	-.0996	-.0138	.0068	.0021	-.1087	95	.0244	-.1331
10-14	30,000	.48	4.7	-3.1	1.3	2.9	-.1058	-.0147	.0056	.0024	-.1173	79	.0199	-.1372
10-13	30,000	.53	7.2	-2.8	1.3	5.7	-.0890	-.0124	.0055	.0020	-.0979	77	.0161	-.1137
4-5	30,000	.54	7.9	-2.8	1.3	6.4	-.0855	-.0116	.0052	.0019	-.0918	95	.0202	-.1120
10-12	30,000	.56	8.4	-2.6	1.4	7.2	-.0799	-.0111	.0057	.0017	-.0870	77	.0144	-.1014
4-6	30,000	.60	13.0	-2.1	.7	11.6	-.0562	-.0078	.0013	.0018	-.0645	92	.0161	-.0806
4-7	30,000	.64	13.5	-2.0	.6	12.1	-.0590	-.0082	.0009	.0016	-.0679	90	.0132	-.0811
4-8	30,000	.70	14.0	-1.9	.8	12.9	-.0628	-.0087	.0017	.0012	-.0710	84	.0103	-.0813
4-9	30,000	.72	15.1	-1.8	1.0	14.3	-.0624	-.0087	.0023	.0013	-.0701	86	.0095	-.0796
4-10	30,000	.74	12.4	-2.1	1.1	11.4	-.0768	-.0107	.0017	.0012	-.0870	84	.0087	-.0957
10-10	30,000	.74	11.8	-2.1	1.4	11.1	-.0788	-.0109	.0035	.0014	-.0876	72	.0076	-.0952
4-11	30,000	.76	16.8	-1.5	1.2	16.5	-.0519	-.0072	.0008	.0011	-.0594	92	.0086	-.0680
4-12	30,000	.78	62.8	4.9	0	67.7	.0756	.0105	-.0032	.0011	.0818	97	.0090	.0728

TABLE IV.- SUMMARY OF PITCHING-MOMENT CHARACTERISTICS

FOR CONFIGURATION B IN GRADUAL MANEUVERS

(a) Lower C_{N_A} range

(1)	(2)	(3)	(4)	(5)	(6)	(7)	(8)	(9)	(10)	(11)	(12)	(13)	(14)	(15)
Flight and run	Approximate altitude	Mach number	x_{ac_m}	$\Delta x_{ac_{area}}$	Δx_{ac_δ}	x_{ac}	$C_{m_{O_m}}$	$\Delta C_{m_{O_{area}}}$	$\Delta C_{m_{O_\delta}}$	$\Delta C_{m_{O_{thrust}}}$	$C_{m_{O_c}}$	$\frac{\Delta T}{C_F}$,	$\Delta C_{m_{O_{\Delta T}}}$	C_{m_O}
15-17	15,000	0.35	18.2	-1.3	1.0	17.9	-0.0130	-0.0018	0.0016	0.0018	-0.0150	35	0.0090	-0.0240
15-16	15,000	.36	18.1	-1.3	.9	17.7	-.0158	-.0022	.0011	.0016	-.0185	35	.0081	-.0266
15-15	15,000	.38	17.8	-1.3	.9	17.4	-.0176	-.0024	.0015	.0016	-.0201	34	.0071	-.0272
15-14	15,000	.40	18.7	-1.2	.9	18.4	-.0131	-.0018	.0011	.0016	-.0154	31	.0059	-.0213
15-18	15,000	.40	19.2	-1.1	.9	19.0	-.0117	-.0016	.0014	.0016	-.0135	34	.0064	-.0199
15-13	15,000	.45	18.1	-1.3	.9	17.7	-.0166	-.0023	.0013	.0015	-.0191	29	.0045	-.0236
15-12	15,000	.49	18.7	-1.2	.9	18.4	-.0169	-.0024	.0013	.0015	-.0195	26	.0033	-.0228
15-11	15,000	.53	18.7	-1.2	1.0	18.5	-.0184	-.0025	.0014	.0013	-.0208	24	.0026	-.0234
15-10	15,000	.57	18.3	-1.3	1.0	18.0	-.0194	-.0027	.0014	.0014	-.0221	20	.0019	-.0240
15-9	15,000	.60	18.7	-1.2	1.1	18.6	-.0199	-.0028	.0016	.0012	-.0223	18	.0015	-.0238
15-8	15,000	.62	18.3	-1.3	1.1	18.1	-.0202	-.0028	.0018	.0014	-.0226	18	.0015	-.0241
15-7	15,000	.64	18.4	-1.3	1.1	18.2	-.0208	-.0029	.0017	.0013	-.0233	16	.0012	-.0245
15-6	15,000	.66	18.9	-1.2	1.1	18.8	-.0204	-.0028	.0017	.0013	-.0228	14	.0010	-.0238
15-5	15,000	.68	19.1	-1.2	1.2	19.1	-.0209	-.0028	.0017	.0012	-.0232	11	.0007	-.0239
15-4	15,000	.70	18.6	-1.3	1.3	18.6	-.0248	-.0034	.0019	.0012	-.0275	13	.0008	-.0283
15-3	15,000	.71	18.6	-1.3	1.3	18.6	-.0277	-.0039	.0016	.0011	-.0311	10	.0006	-.0317
15-2	15,000	.74	19.8	-1.1	1.4	20.1	-.0299	-.0042	.0017	.0011	-.0335	15	.0008	-.0343
15-1A	15,000	.76	16.7	-1.6	1.1	16.2	-.0372	-.0052	.0015	.0010	-.0419	23	.0012	-.0431
15-1B	15,000	.76	15.6	-1.8	1.3	15.1	-.0405	-.0056	.0011	.0010	-.0460	23	.0012	-.0472
13-1	22,500	.36	16.9	-1.6	.9	16.2	-.0054	-.0008	.0019	.0026	-.0069	68	.0226	-.0295
13-2	22,500	.36	17.2	-1.5	.8	16.5	-.0031	-.0004	.0012	.0025	-.0048	67	.0214	-.0262
13-3	22,500	.38	17.2	-1.5	.9	16.6	-.0041	-.0006	.0025	.0029	-.0051	67	.0199	-.0250
13-4	22,500	.40	17.7	-1.4	.8	17.1	-.0075	-.0012	.0008	.0018	-.0097	67	.0176	-.0273
13-5	22,500	.44	18.1	-1.4	.8	17.5	-.0072	-.0010	.0009	.0017	-.0090	65	.0141	-.0231
13-6	22,500	.48	19.1	-1.2	.8	18.8	-.0050	-.0007	.0014	.0016	-.0059	63	.0113	-.0172
13-7	22,500	.53	19.5	-1.2	.9	19.2	-.0073	-.0010	.0013	.0015	-.0085	61	.0091	-.0176
13-8	22,500	.57	19.2	-1.2	.9	18.9	-.0098	-.0014	.0014	.0014	-.0112	58	.0074	-.0186
13-9	22,500	.62	19.1	-1.2	1.0	18.9	-.0137	-.0019	.0015	.0013	-.0154	56	.0061	-.0215
13-10	22,500	.66	19.0	-1.2	1.0	18.8	-.0177	-.0025	.0015	.0013	-.0200	52	.0049	-.0249
13-11	22,500	.68	19.7	-1.1	1.1	19.7	-.0174	-.0024	.0016	.0013	-.0195	49	.0044	-.0239
13-12	22,500	.70	18.8	-1.2	1.2	18.8	-.0209	-.0029	.0016	.0012	-.0234	49	.0043	-.0277
13-13	22,500	.72	19.1	-1.2	1.2	19.1	-.0256	-.0036	.0015	.0012	-.0289	50	.0041	-.0330
13-14	22,500	.74	20.1	-1.0	1.3	20.4	-.0272	-.0038	.0015	.0012	-.0307	44	.0033	-.0340
13-15	22,500	.75	17.6	-1.4	1.2	17.4	-.0352	-.0049	.0011	.0011	-.0401	46	.0033	-.0434
13-16	22,500	.77	14.1	-1.8	1.4	13.7	-.0363	-.0050	.0011	.0011	-.0413	50	.0033	-.0446
11-2	30,000	.42	16.6	-1.6	1.2	16.2	-.0038	-.0005	.0046	.0027	-.0024	90	.0298	-.0322
11-3	30,000	.45	18.1	-1.4	1.0	17.7	.0021	.0003	.0027	.0025	.0026	90	.0254	-.0228
11-4	30,000	.48	18.7	-1.3	.9	18.3	.0031	.0004	.0023	.0023	.0035	91	.0229	-.0194
11-5	30,000	.51	18.5	-1.3	.8	18.0	-.0027	-.0004	.0015	.0019	-.0035	91	.0203	-.0238
11-6	30,000	.55	18.6	-1.3	.8	18.2	-.0044	-.0006	.0017	.0019	-.0052	91	.0181	-.0233
11-7	30,000	.58	19.8	-1.1	.9	19.6	-.0025	-.0003	.0016	.0017	-.0029	90	.0153	-.0182
11-8	30,000	.61	19.5	-1.1	.9	19.3	-.0083	-.0011	.0019	.0016	-.0091	88	.0140	-.0231
11-9	30,000	.65	19.6	-1.1	1.0	19.5	-.0108	-.0015	.0018	.0014	-.0119	85	.0117	-.0236
11-10	30,000	.68	19.1	-1.2	1.0	18.9	-.0163	-.0023	.0019	.0014	-.0181	85	.0107	-.0288
11-11	30,000	.70	19.0	-1.2	1.0	18.9	-.0192	-.0027	.0017	.0013	-.0215	82	.0099	-.0314
11-12	30,000	.72	19.6	-1.1	1.0	19.5	-.0199	-.0028	.0016	.0013	-.0224	81	.0093	-.0317
11-13	30,000	.74	19.0	-1.2	1.2	19.0	-.0299	-.0042	.0017	.0012	-.0336	80	.0084	-.0420
11-14	30,000	.76	14.7	-1.8	1.7	14.3	-.0391	-.0054	.0020	.0012	-.0453	79	.0078	-.0531
11-15	30,000	.78	11.9	-2.1	1.6	11.4	-.0355	-.0049	.0009	.0011	-.0406	81	.0075	-.0481

TABLE IV.- SUMMARY OF PITCHING-MOMENT CHARACTERISTICS

FOR CONFIGURATION B IN GRADUAL MANEUVERS - Concluded

(b) Upper C_{N_A} range

(1)	(2)	(3)	(4)	(5)	(6)	(7)	(8)	(9)	(10)	(11)	(12)	(13)	(14)	(15)
Flight and run	Approximate altitude	Mach number	x_{ac_m}	$\Delta x_{ac_{area}}$	Δx_{ac_δ}	x_{ac}	$C_{m_{O_m}}$	$\Delta C_{m_{O_{area}}}$	$\Delta C_{m_{O_\delta}}$	$\Delta C_{m_{O_{thrust}}}$	$C_{m_{O_c}}$	$\frac{\Delta T}{\sigma_F}$,	$\Delta C_{m_{O_{\Delta T}}}$	C_{m_O}
11-1	30,000	0.38	3.6	-3.4	2.9	3.1	-0.1132	-0.0157	0.0200	0.0029	-0.1118	85	0.0350	-0.1468
11-2	30,000	.42	6.9	-2.9	2.2	6.2	-.0752	-.0104	.0121	.0027	-.0762	90	.0298	-.1060
11-3	30,000	.45	5.0	-3.9	2.4	3.5	-.0931	-.0132	.0132	.0025	-.0956	90	.0254	-.1210
11-4	30,000	.49	7.6	-2.8	2.0	5.8	-.0715	-.0099	.0097	.0023	-.0740	91	.0229	-.0969
11-5	30,000	.51	6.9	-2.9	1.9	5.9	-.0760	-.0106	.0090	.0019	-.0795	91	.0203	-.0998
11-6	30,000	.55	10.5	-2.4	1.2	9.3	-.0526	-.0073	.0039	.0019	-.0579	91	.0181	-.0760
11-7	30,000	.58	13.2	-2.0	1.0	12.2	-.0381	-.0053	.0024	.0017	-.0427	90	.0153	-.0580
11-8	30,000	.62	15.1	-1.8	.8	14.1	-.0296	-.0041	.0010	.0016	-.0343	88	.0140	-.0483
11-9	30,000	.65	15.4	-1.7	.6	14.3	-.0310	-.0043	.0002	.0014	-.0365	85	.0117	-.0482
11-10	30,000	.68	16.2	-1.6	.7	15.3	-.0286	-.0040	.0007	.0014	-.0333	85	.0107	-.0440
11-11	30,000	.70	16.3	-1.6	.6	15.3	-.0304	-.0042	.0007	.0013	-.0353	82	.0099	-.0452
11-12	30,000	.72	17.2	-1.4	.8	16.6	-.0287	-.0040	.0011	.0013	-.0329	81	.0093	-.0422
11-13	30,000	.74	15.3	-1.7	1.0	14.6	-.0419	-.0058	.0014	.0012	-.0475	80	.0084	-.0559
11-14	30,000	.76	7.2	-2.8	.6	5.0	-.0642	-.0089	-.0014	.0012	-.0755	79	.0078	-.0833
11-15	30,000	.78	28.6	.2	.5	29.3	.0068	.0009	-.0019	.0011	.0047	81	.0075	-.0028
13-7	22,500	.53	13.3	-2.0	1.1	12.4	-.0411	-.0057	.0028	.0015	-.0455	61	.0091	-.0546
13-8	22,500	.57	15.2	-1.7	.9	14.4	-.0305	-.0042	.0011	.0014	-.0348	58	.0074	-.0422
13-9	22,500	.62	16.6	-1.5	.8	15.9	-.0248	-.0035	.0004	.0013	-.0292	56	.0061	-.0353
13-10	22,500	.66	16.2	-1.6	.8	15.4	-.0290	-.0040	.0004	.0013	-.0339	52	.0049	-.0388
13-11	22,500	.68	15.4	-1.7	.7	14.4	-.0340	-.0047	.0001	.0013	-.0399	49	.0044	-.0443
13-12	22,500	.70	14.6	-1.8	.9	13.7	-.0378	-.0053	.0006	.0012	-.0437	49	.0043	-.0480

TABLE V.- SUMMARY OF PITCHING-MOMENT CHARACTERISTICS

FOR CONFIGURATION A IN ABRUPT MANEUVERS

Flight and run	M	x_{ac}	C_{m_0}	I_y, slug-ft^2	k_y, ft
8-2	0.39	17.5	-0.0533	298,000	12.4
8-3	.45	17.4	-.0582	263,000	11.7
8-14	.50	17.0	-.0513	260,000	12.3
8-4	.50	17.4	-.0560	267,000	11.9
8-5	.55	16.5	-.0561	276,000	12.2
8-6	.61	16.9	-.0587	268,000	12.0
8-13	.66	17.8	-.0563	281,000	12.7
8-7	.66	17.4	-.0604	279,000	12.4
8-8	.69	16.4	-.0625	264,000	12.1
8-9	.71	17.6	-.0672	262,000	12.1
8-10	.73	17.1	-.0711	257,000	12.0
8-11	.75	16.2	-.0760	284,000	12.6
8-12	.75	15.5	-.0751	253,000	12.0

TABLE VI.- SUMMARY OF PITCHING-MOMENT CHARACTERISTICS

FOR CONFIGURATION B IN ABRUPT MANEUVERS

Flight and run	M	x_{ac}	C_{m_0}	I_y, slug-ft^2	k_y, ft	M_e slugs
18-14	0.35	19.1	-0.0186	283,000	12.5	188
18-13	.40	19.2	-.0176	285,000	12.5	211
18-12	.44	19.3	-.0210	285,000	12.5	218
18-18	.45	19.9	-.0192	303,000	13.0	197
18-17	.49	18.7	-.0212	274,000	12.3	180
18-16	.50	18.7	-.0211	282,000	12.5	200
18-11	.50	18.8	-.0228	273,000	12.2	181
18-10	.54	19.0	-.0226	277,000	12.3	187
18-15	.55	18.8	-.0236	272,000	12.3	172
18-9	.58	17.7	-.0234	280,000	12.3	203
18-8	.62	19.0	-.0218	287,000	12.4	191
18-7	.65	19.1	-.0227	282,000	12.3	185
18-6	.67	18.9	-.0255	279,000	12.2	205
18-5	.70	17.6	-.0280	284,000	12.3	198
18-4	.70	18.8	-.0292	269,000	11.9	197
18-3	.72	18.9	-.0311	265,000	11.8	200
18-2	.72	19.1	-.0334	272,000	11.9	175
18-1	.74	19.5	-.0368	278,000	11.9	180

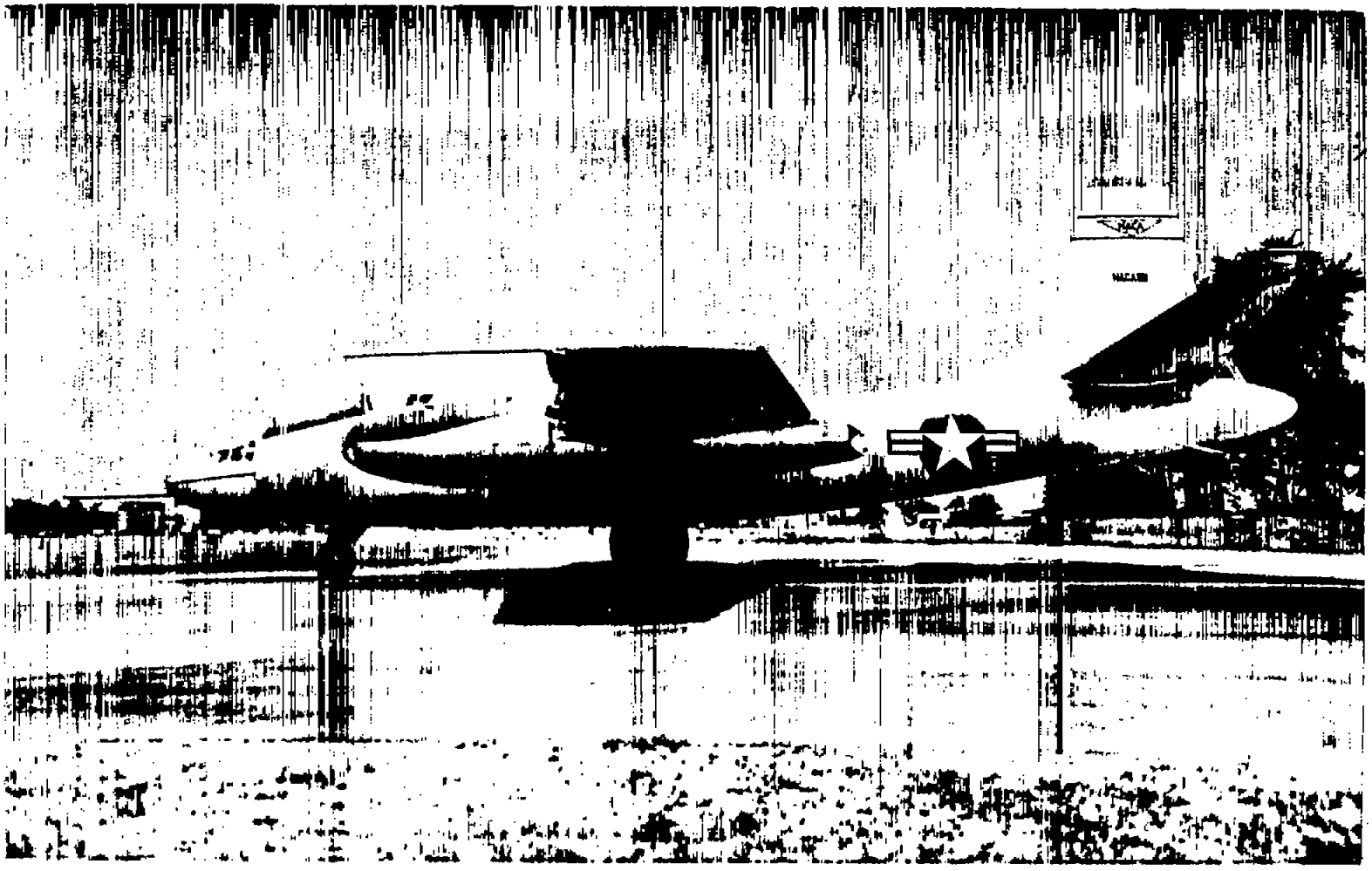

L-71290

Figure 1.- Test airplane, configuration B.

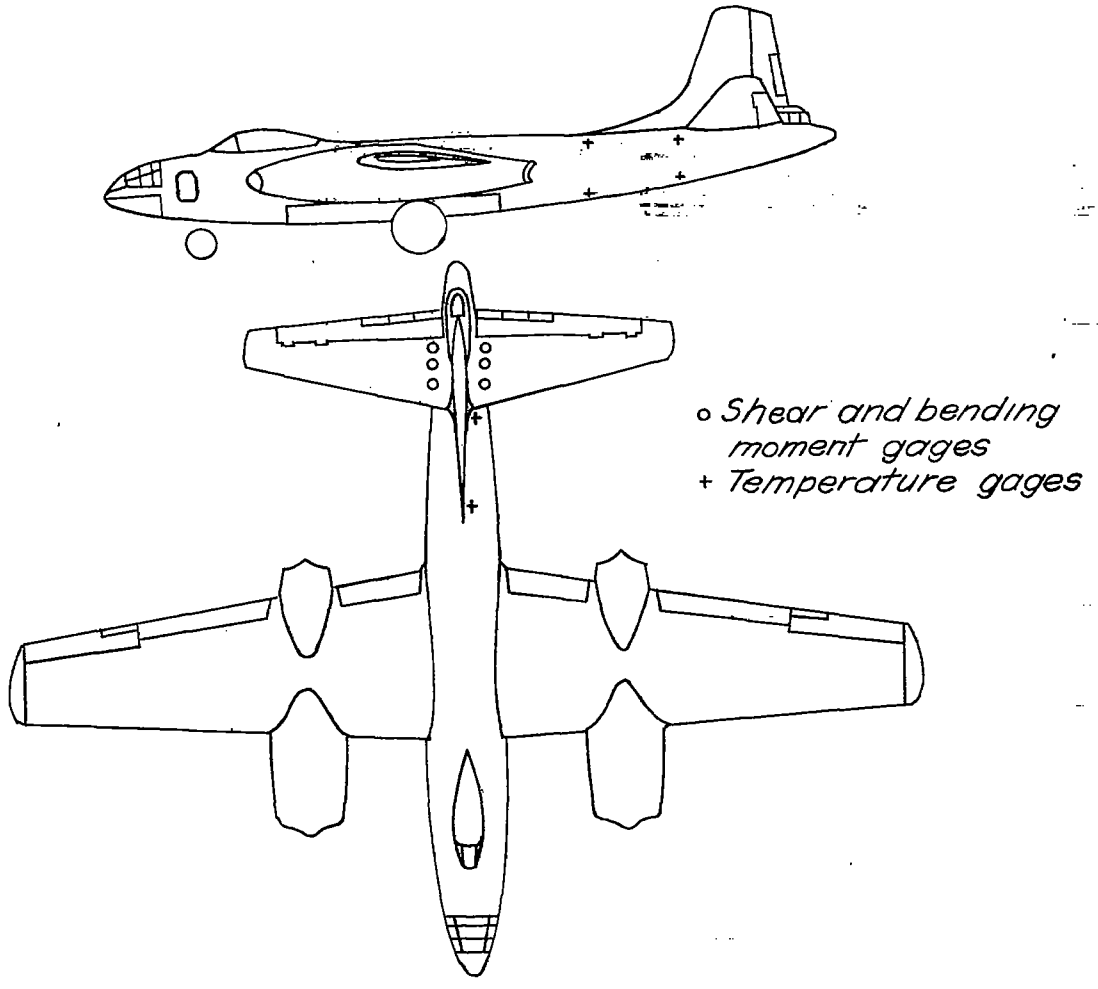

(a) Test airplane showing approximate locations of strain-gage bridges and temperature gages.

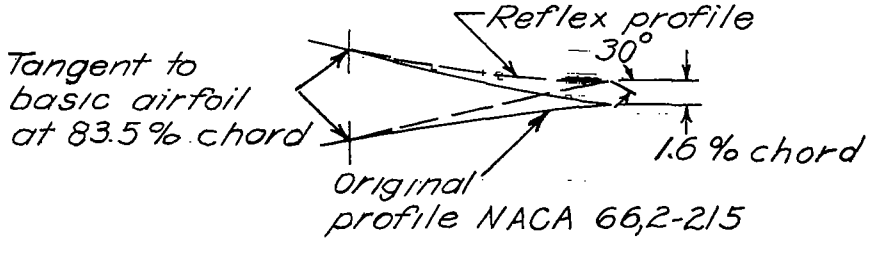

(b) Original and reflexed flap profiles.

Figure 2.- Test airplane with approximate locations of strain-gage bridges and temperature gages, and original (configuration A) and reflexed (configuration B) flap profiles.

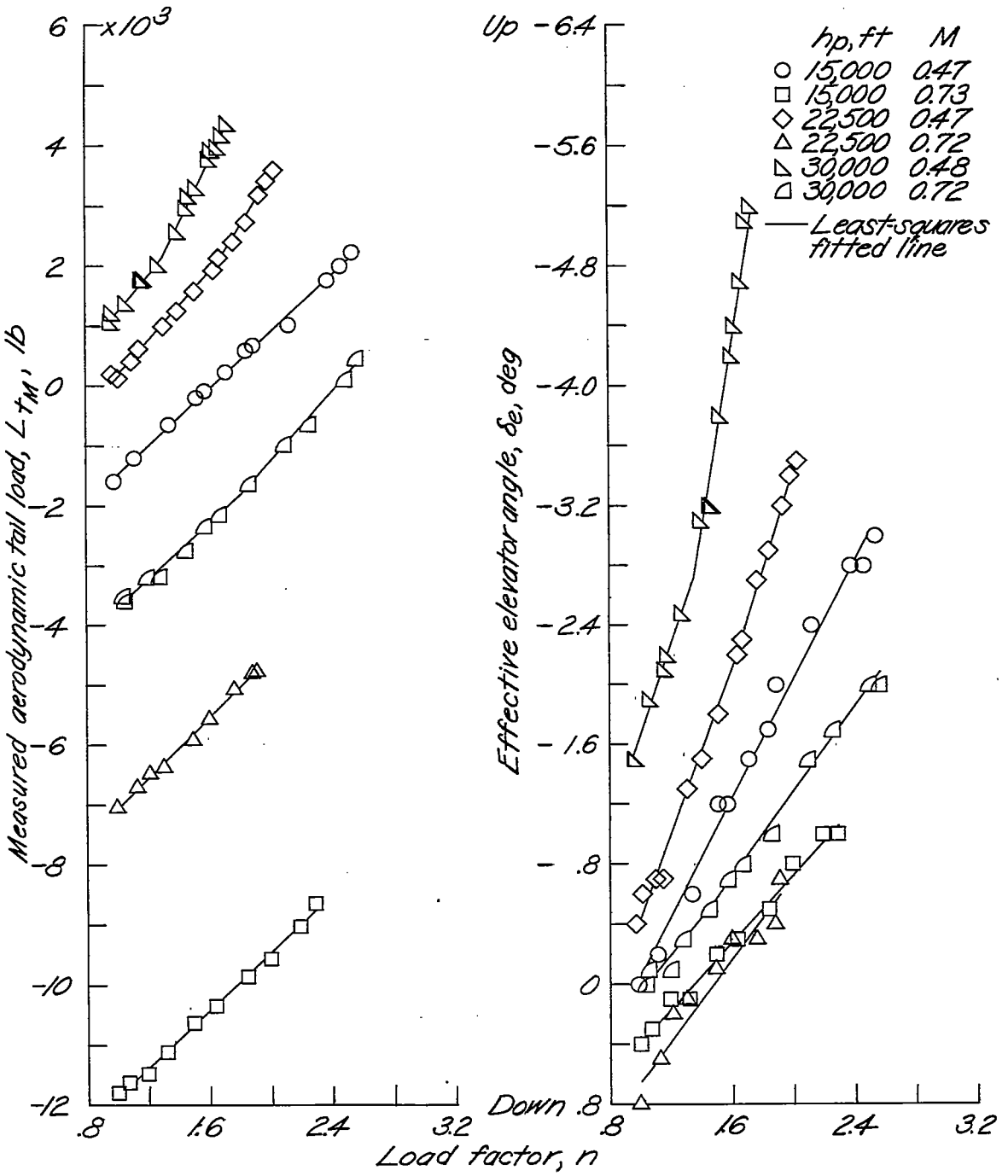

Figure 3.- Examples of basic data for configuration A.

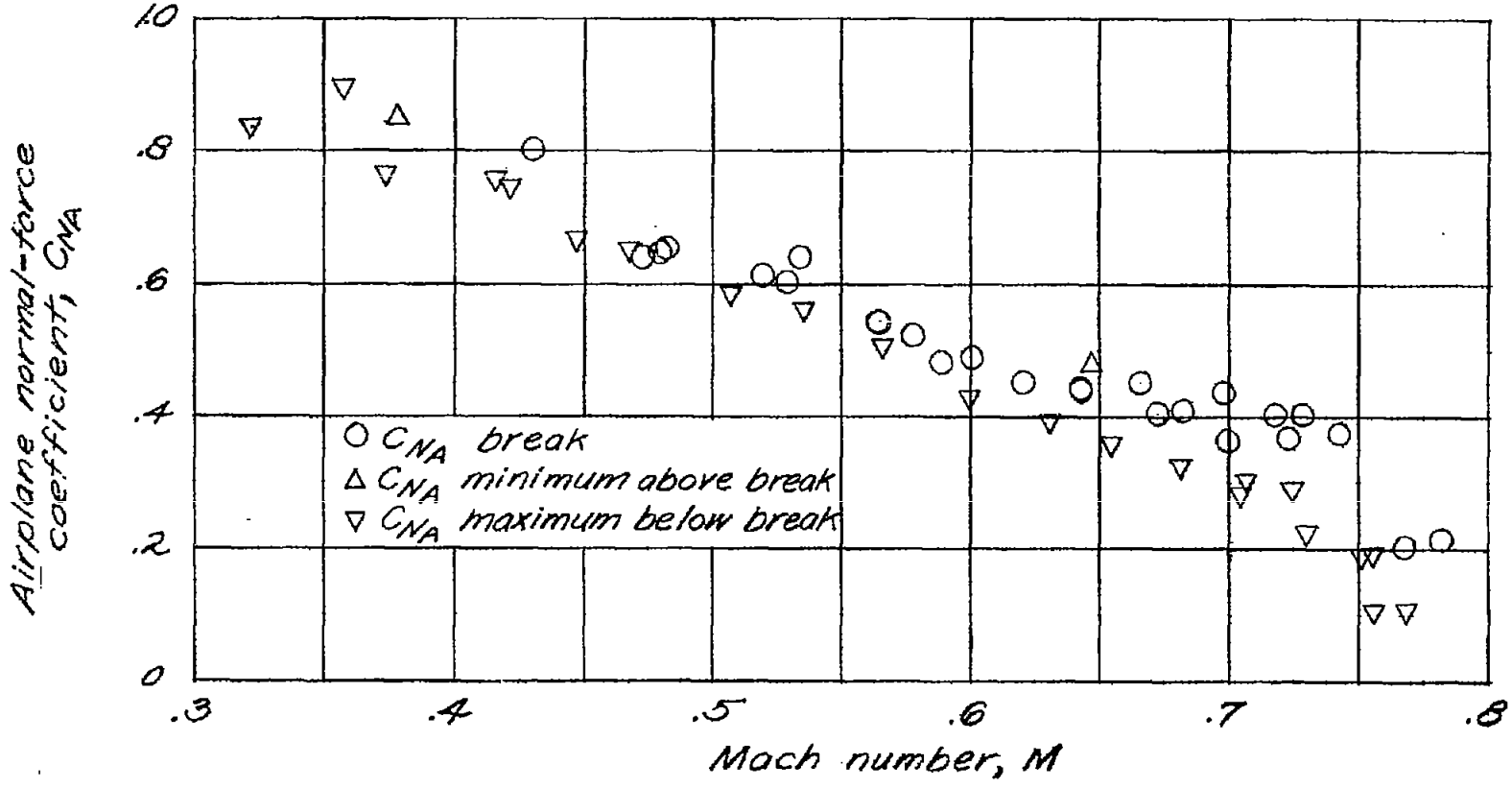

Figure 4.- Normal-force coefficients for aerodynamic-center shift for configuration A.

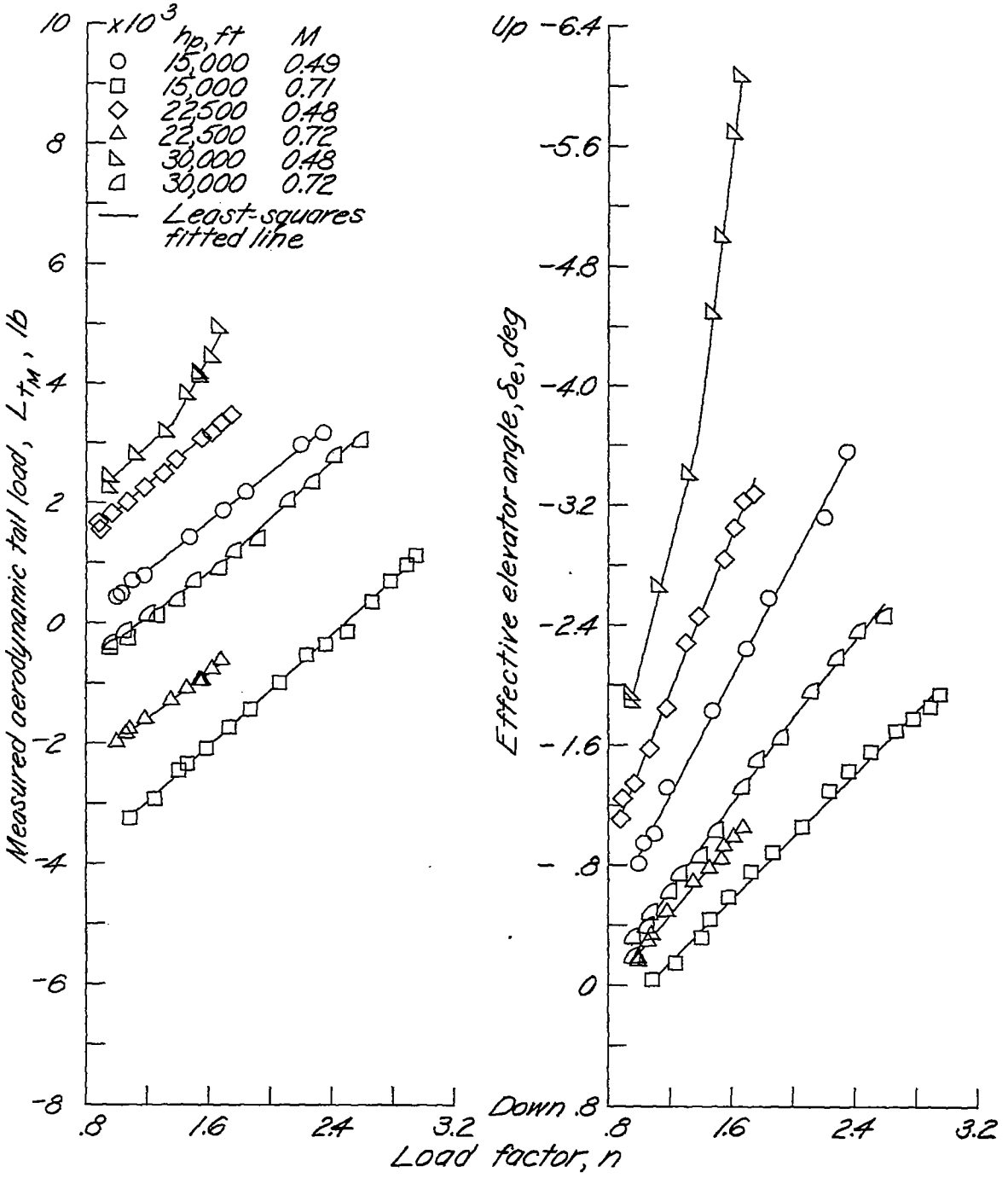

Figure 5.- Examples of basic data for configuration B.

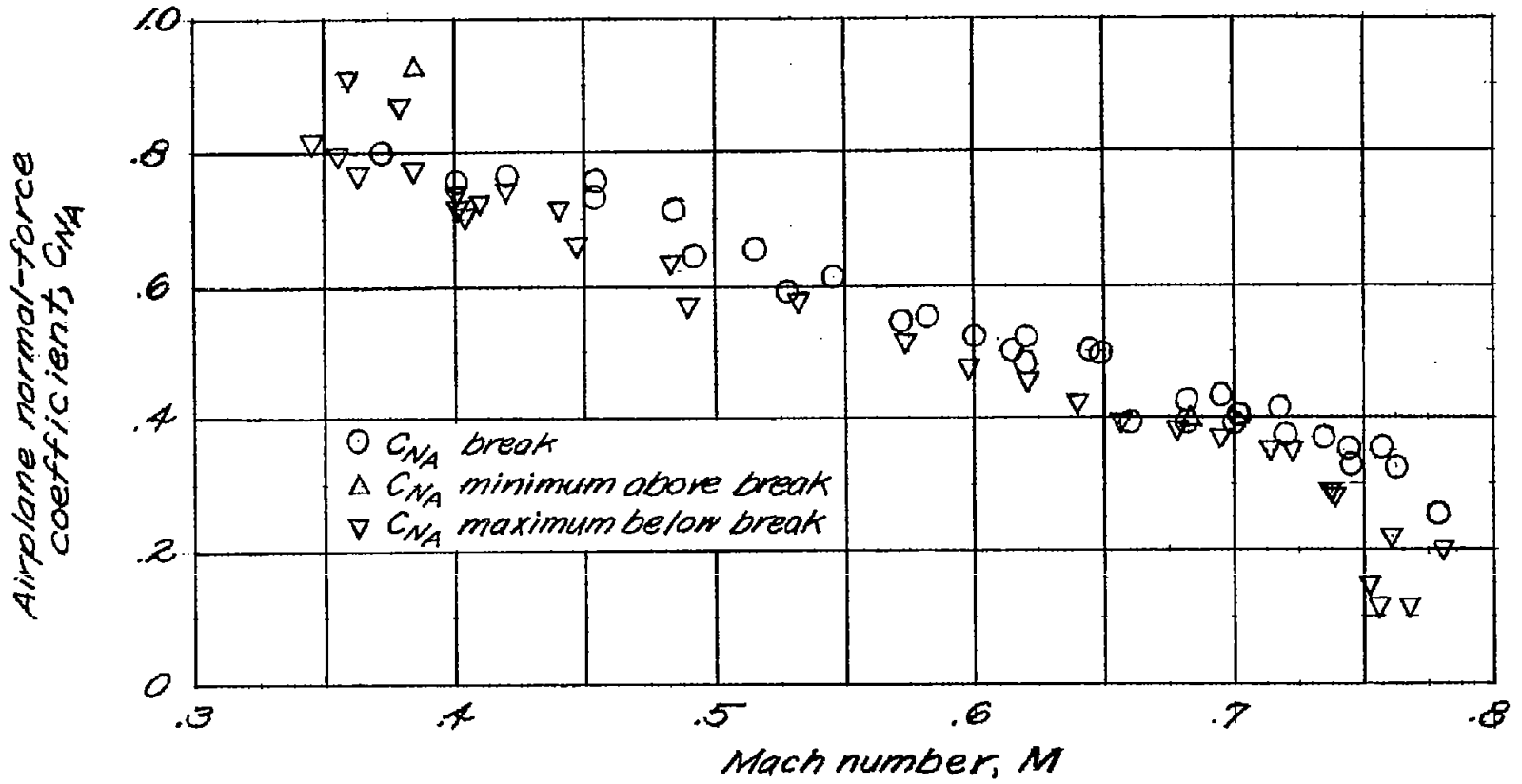

Figure 6.- Normal-force coefficients for aerodynamic-center shift for configuration B.

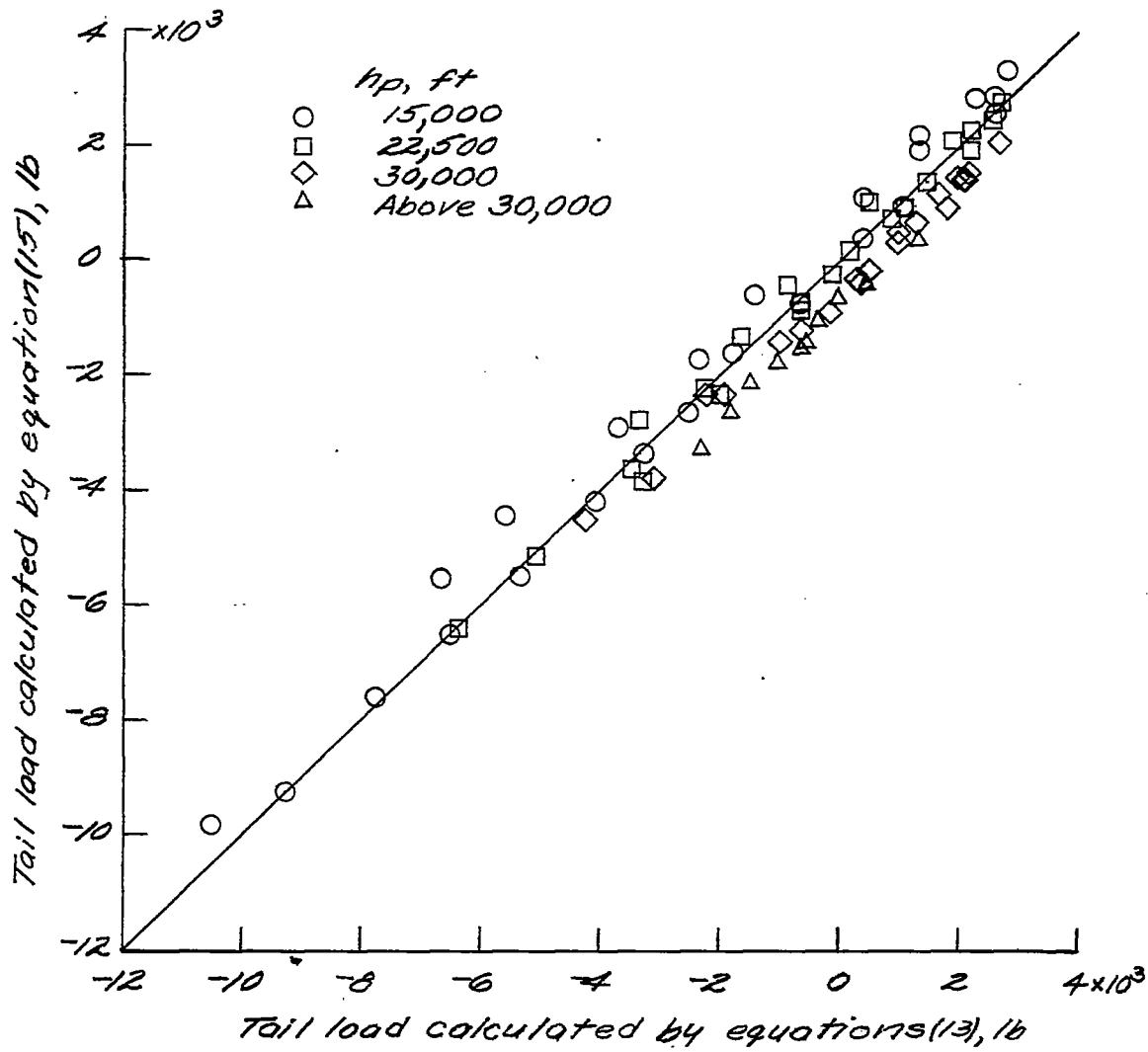

Figure 7.- Comparison of tail loads calculated by equations (13) and (15) for configuration A in lower C_{N_A} range. Without temperature correction term; s = ±552 lb.

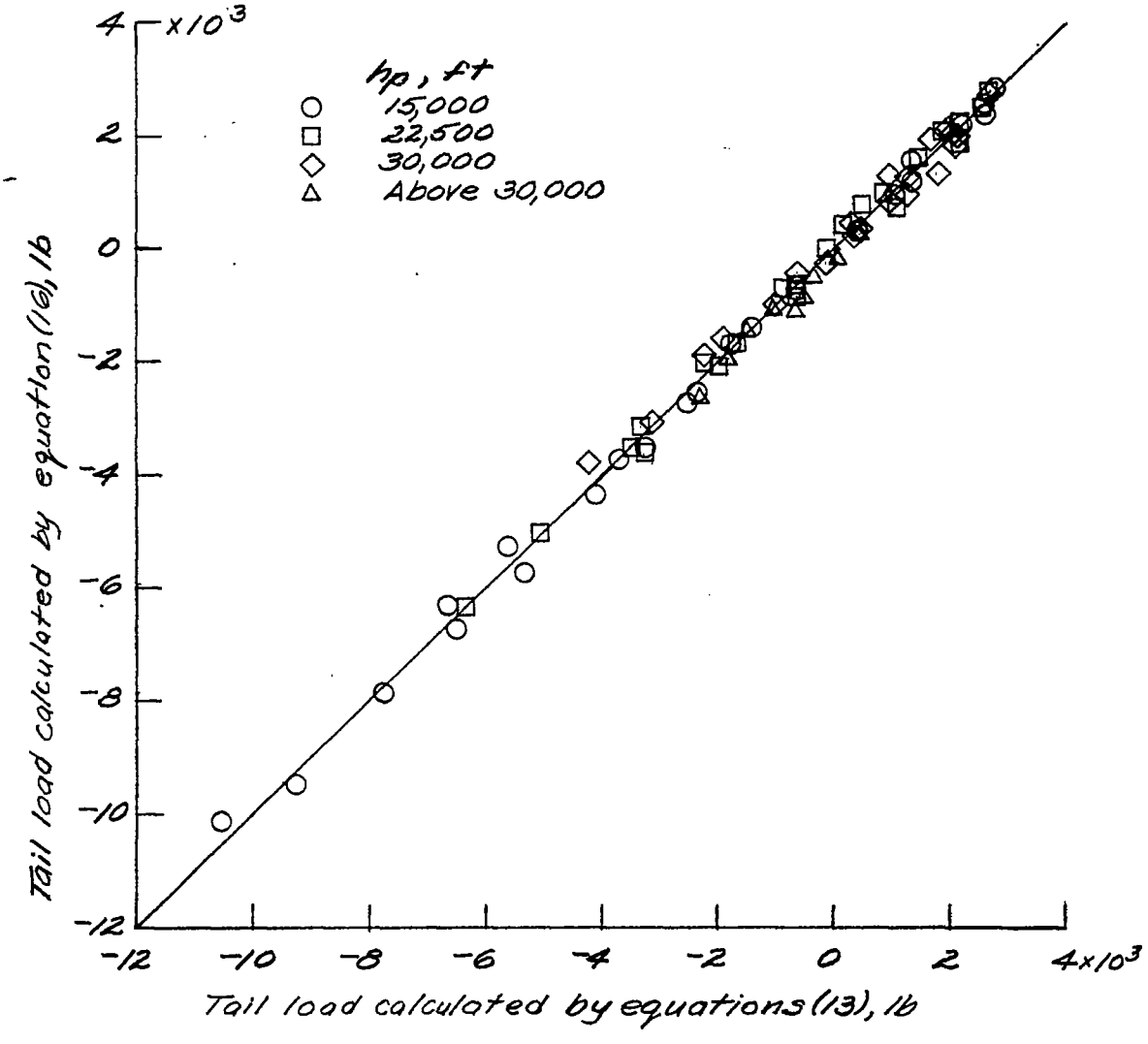

Figure 8.- Comparison of tail loads calculated by equations (13) and (16) for configuration A in lower C_{N_A} range. With temperature correction term; s = ±221 lb.

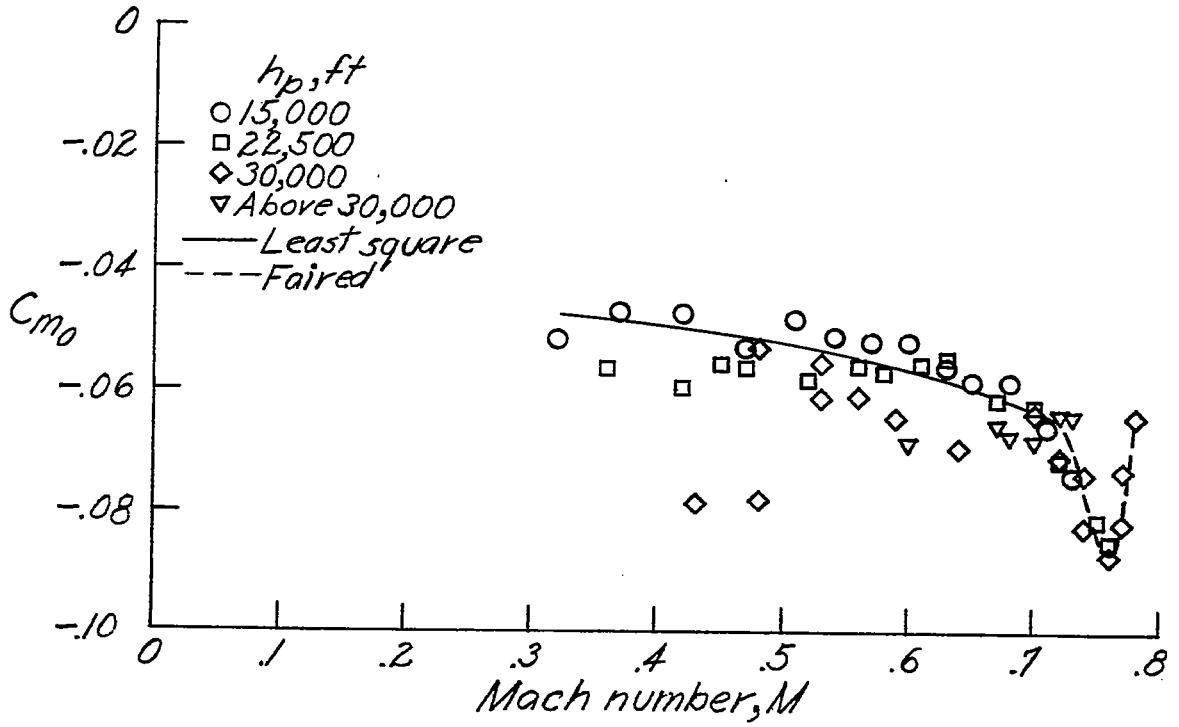

Figure 9.- Wing-fuselage zero-lift pitching-moment coefficient for configuration A in gradual maneuvers in lower C_{N_A} range.

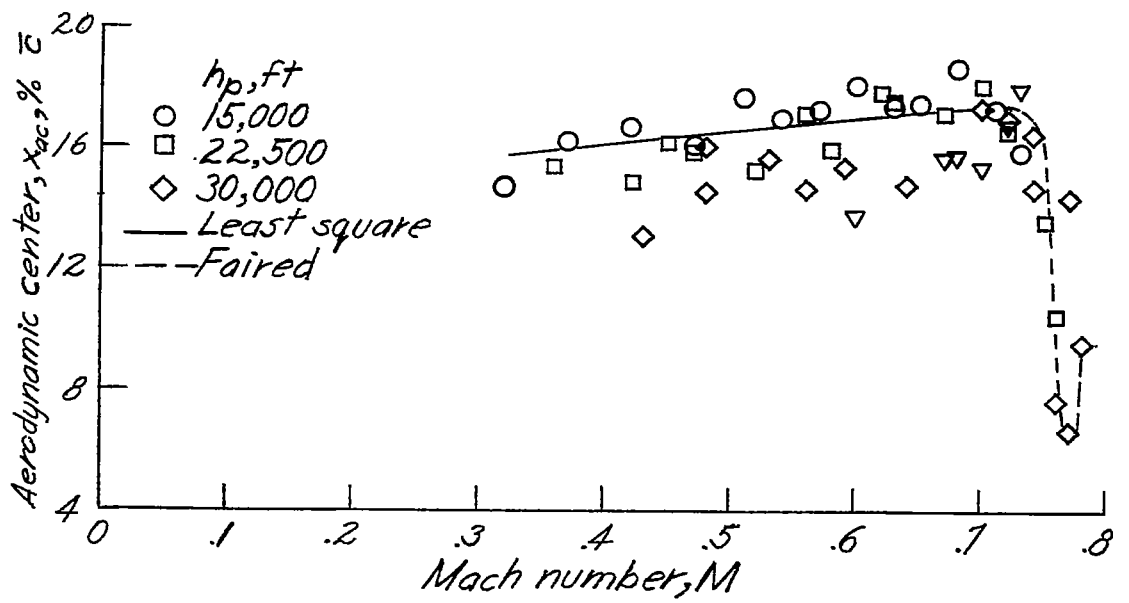

Figure 10.- Wing-fuselage aerodynamic-center position for configuration A in gradual maneuvers in lower C_{N_A} range.

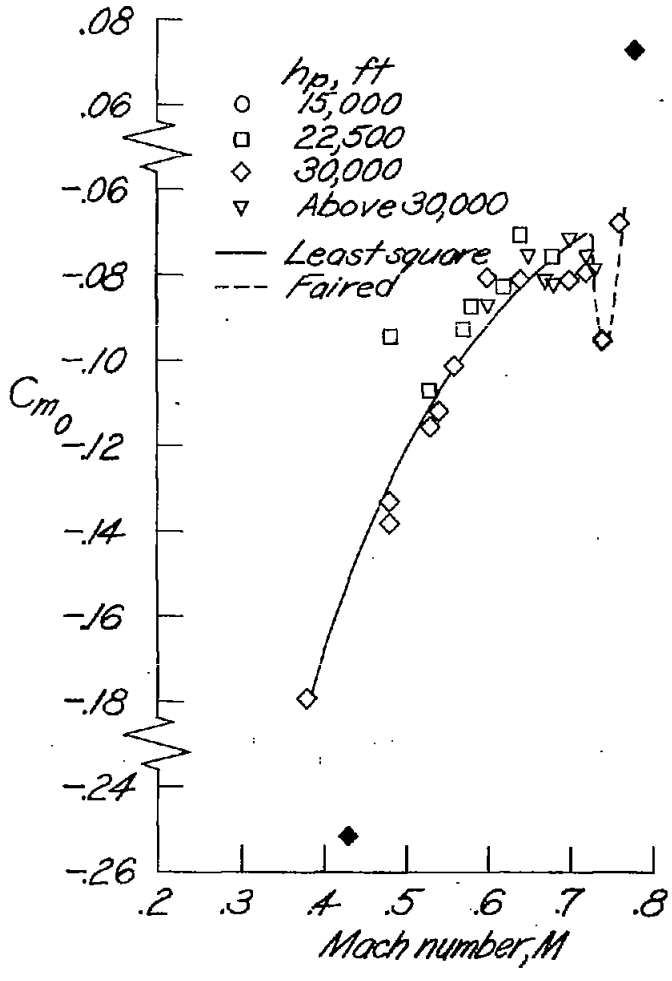

Figure 11.- Wing-fuselage zero-lift pitching-moment coefficient for configuration A in gradual maneuvers in upper C_{N_A} range.

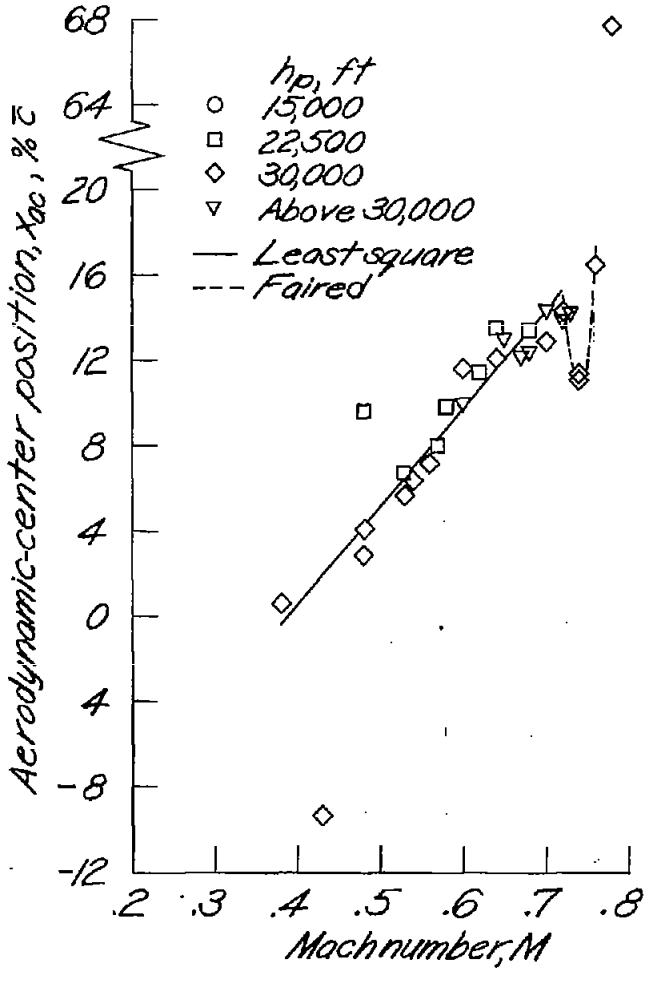

Figure 12.- Wing-fuselage aerodynamic-center position for configuration A in gradual maneuvers in upper C_{N_A} range.

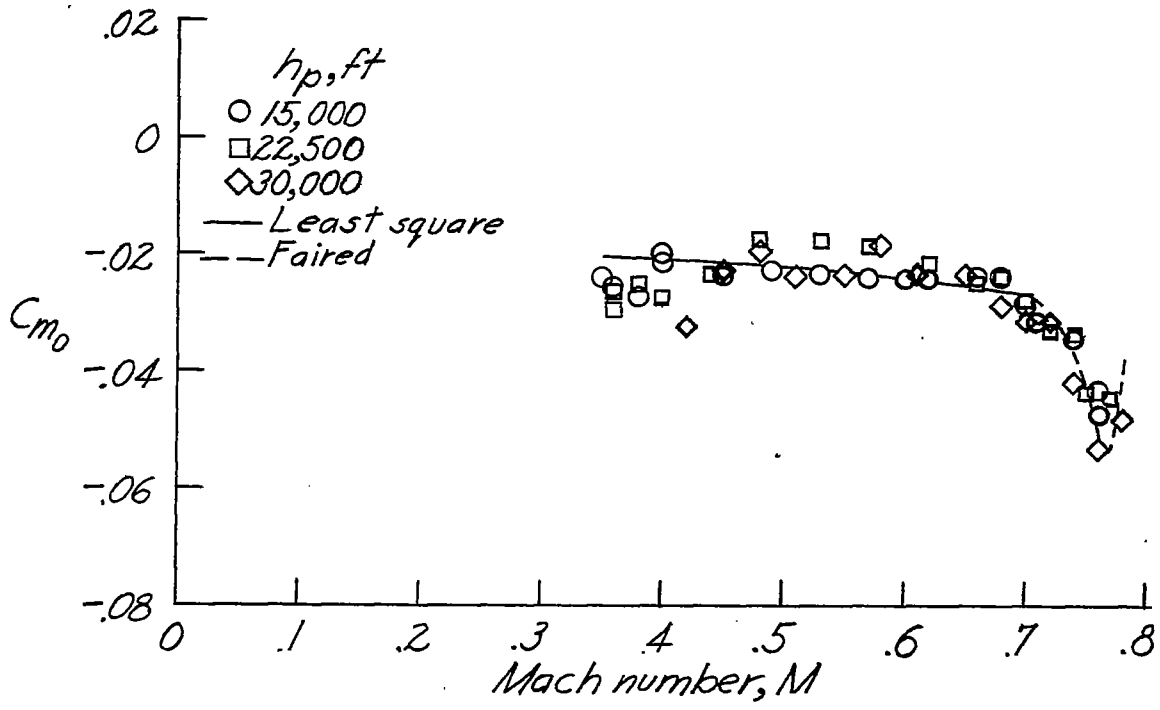

Figure 13.- Wing-fuselage zero-lift pitching-moment coefficient for configuration B in gradual maneuvers in lower C_{N_A} range.

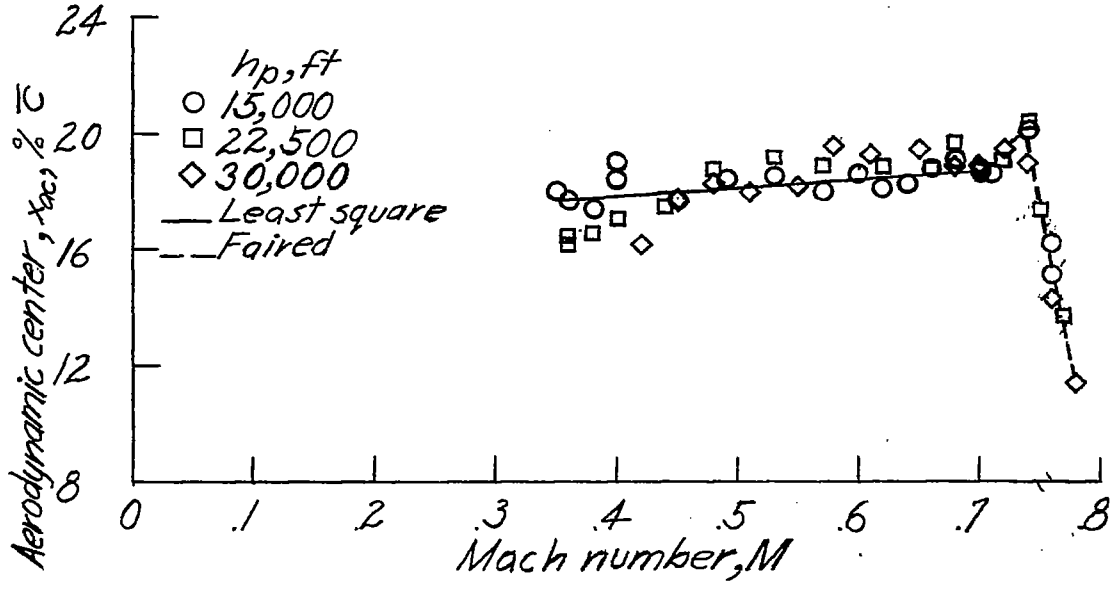

Figure 14.- Wing-fuselage aerodynamic-center position for configuration B in gradual maneuvers in lower C_{N_A} range.

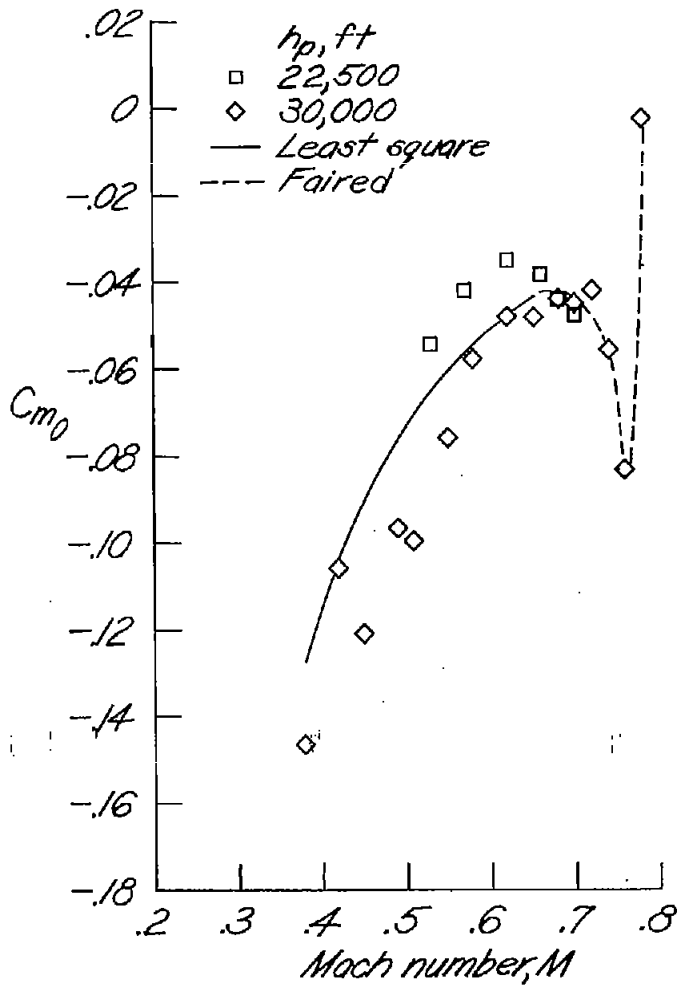

Figure 15.- Wing-fuselage zero-lift pitching-moment coefficient for configuration B in gradual maneuvers in upper C_{N_A} range.

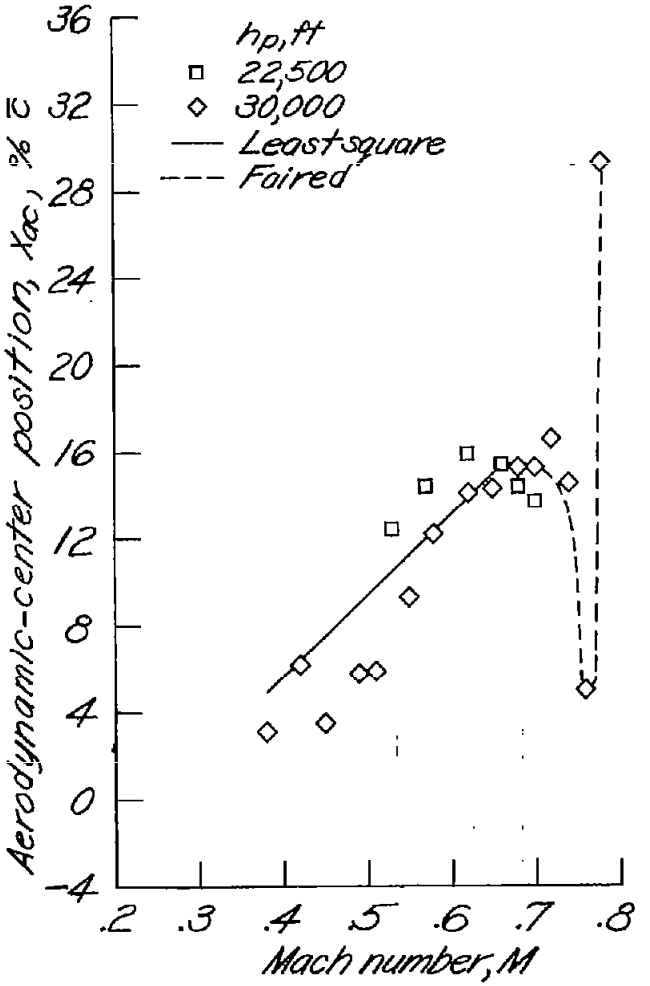

Figure 16.- Wing-fuselage aerodynamic-center position for configuration B in gradual maneuvers in upper C_{N_A} range.

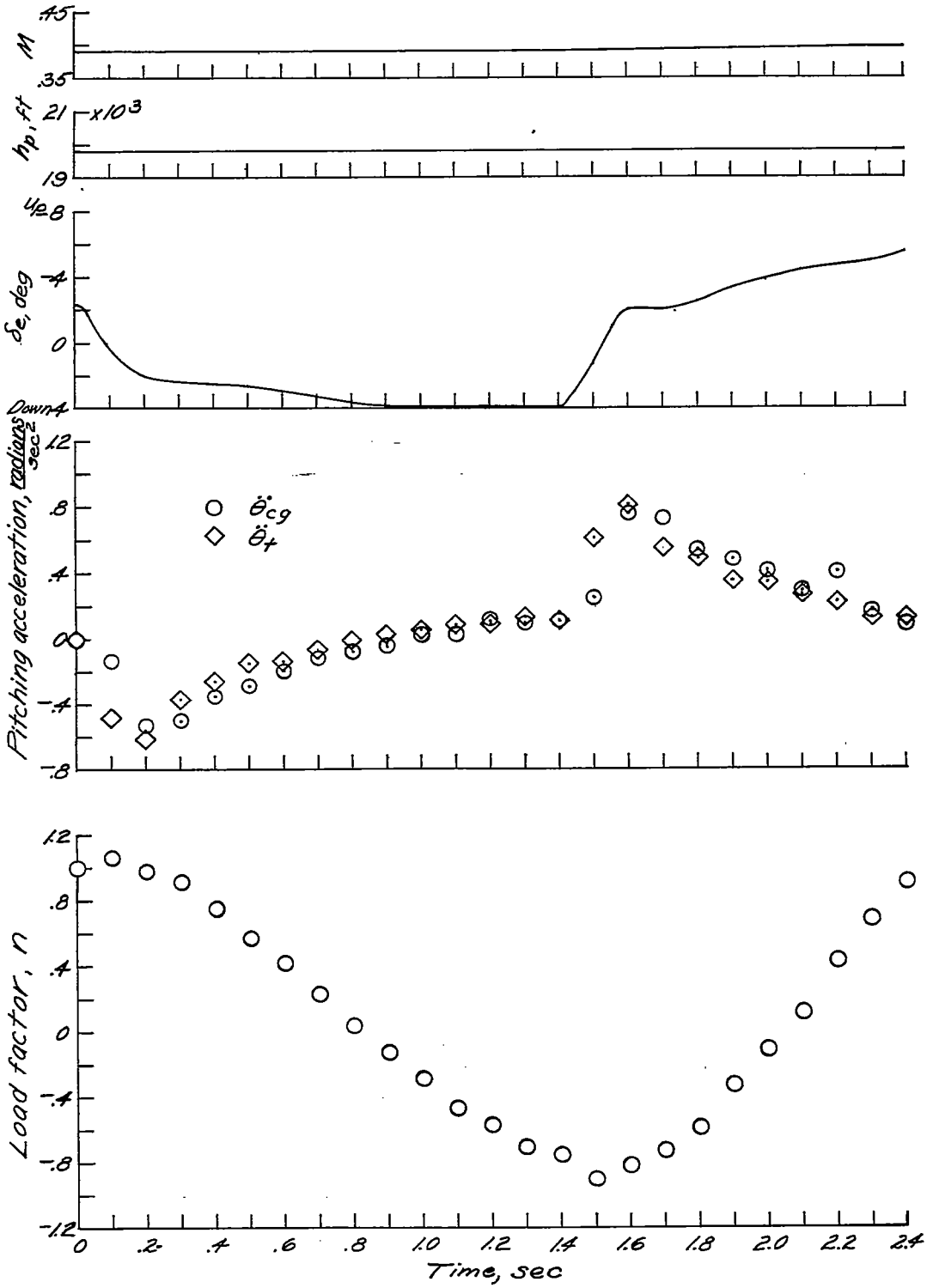

Figure 17.- Time histories of measured quantities and calculated errors of fit for an abrupt push-down pull-up. Configuration A; M = 0.39.

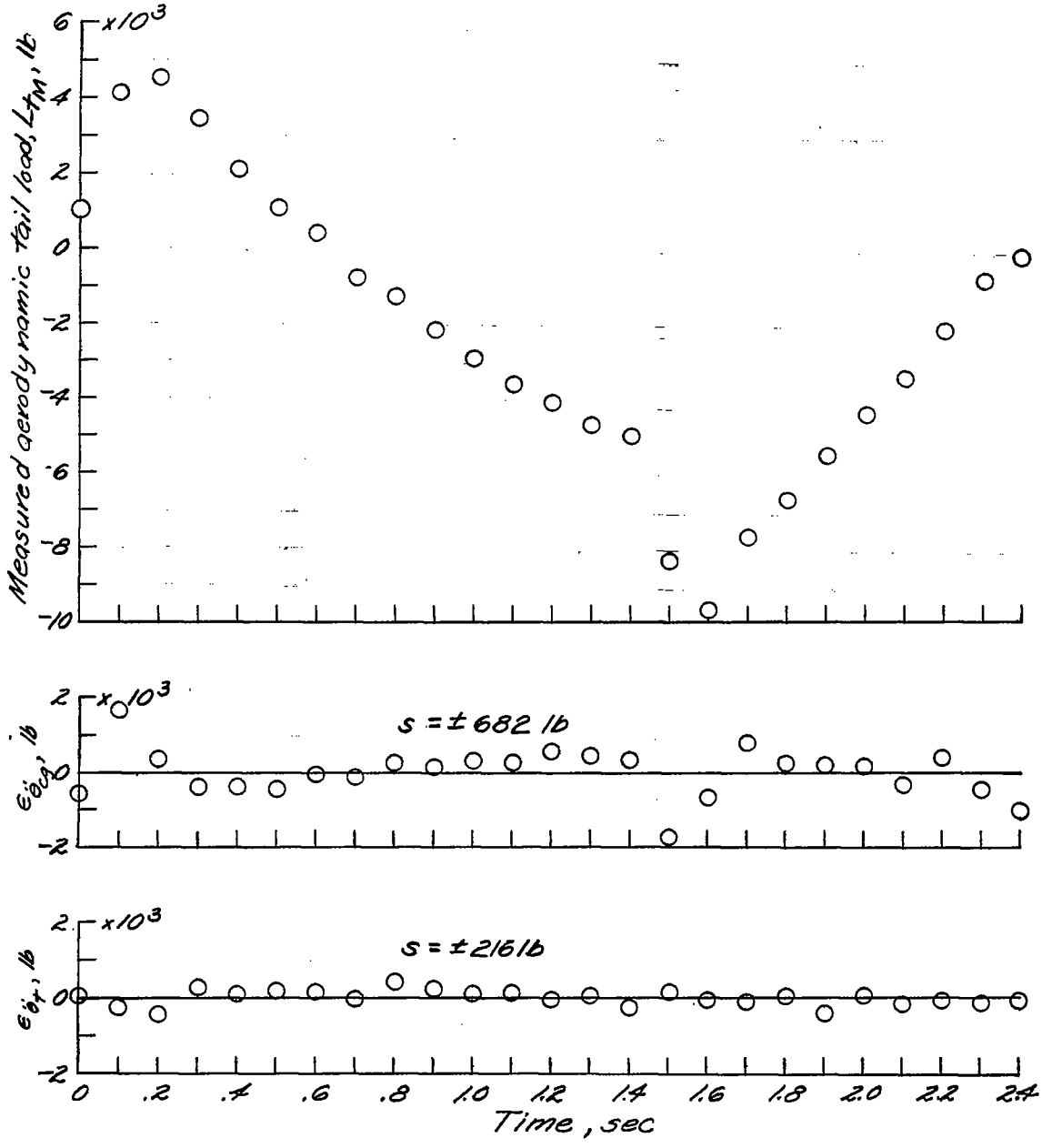

Figure 17.- Concluded.

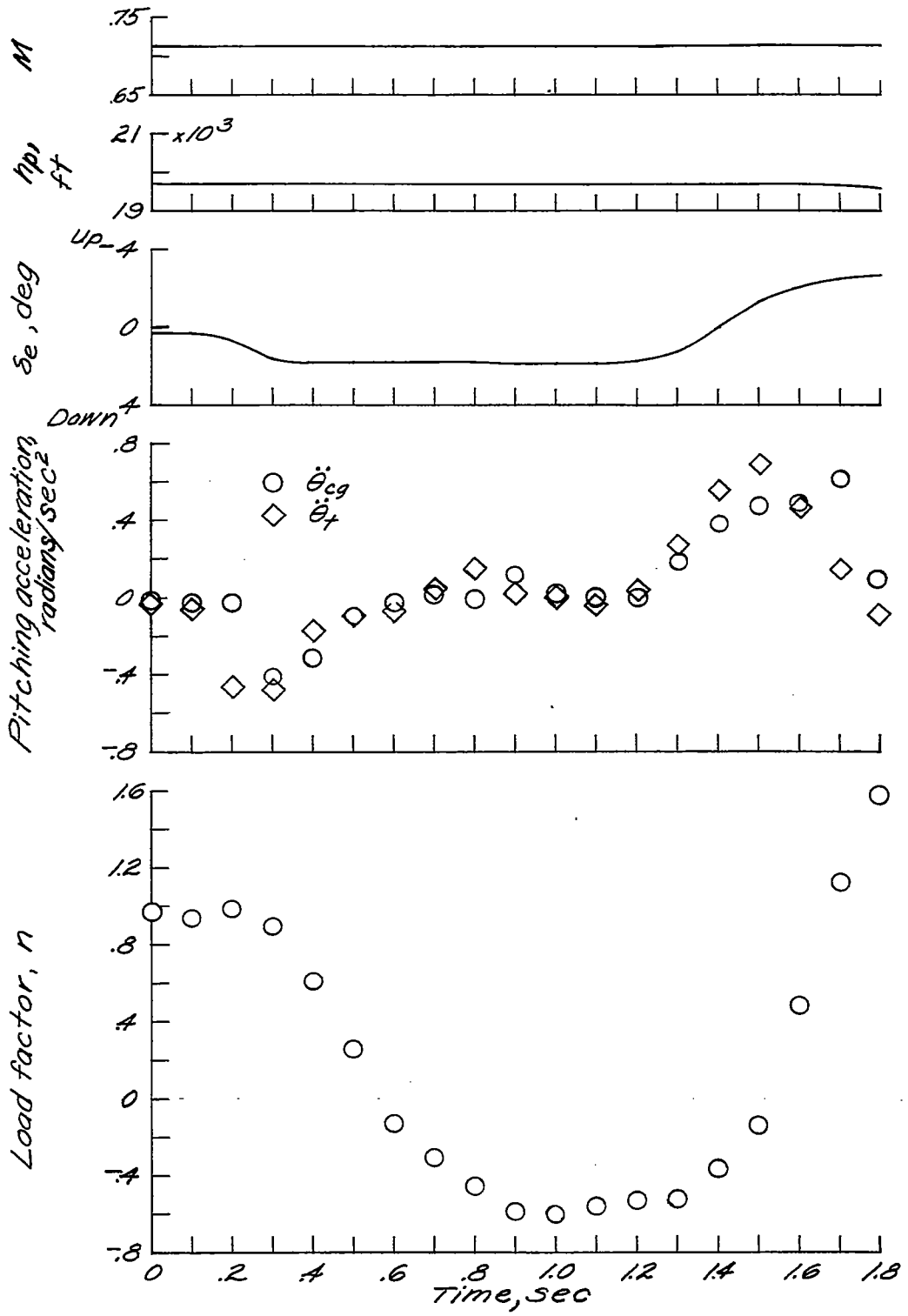

Figure 18.- Time histories of measured quantities and calculated errors of fit for an abrupt push-down pull-up. Configuration A; M = 0.71.

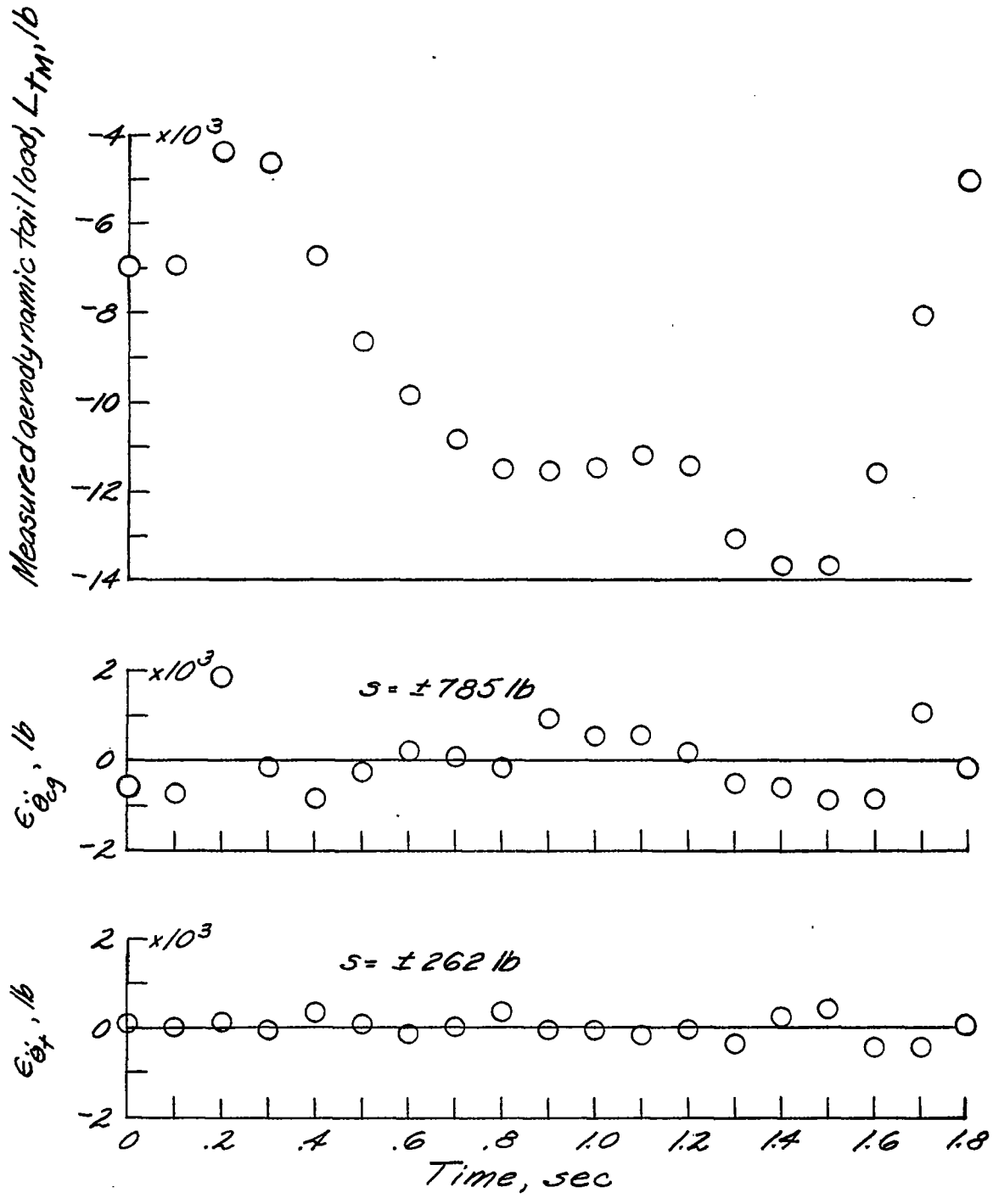

Figure 18.- Concluded.

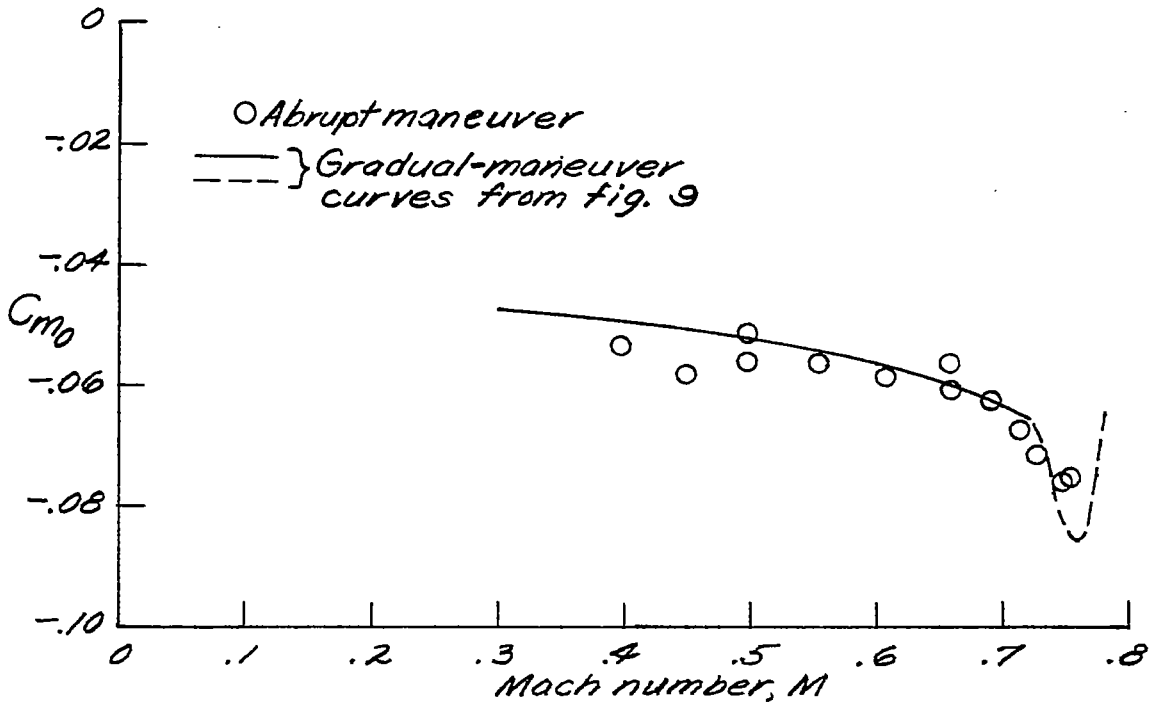

Figure 19.- Wing-fuselage zero-lift pitching-moment coefficient for configuration A in abrupt maneuvers in lower C_{N_A} range.

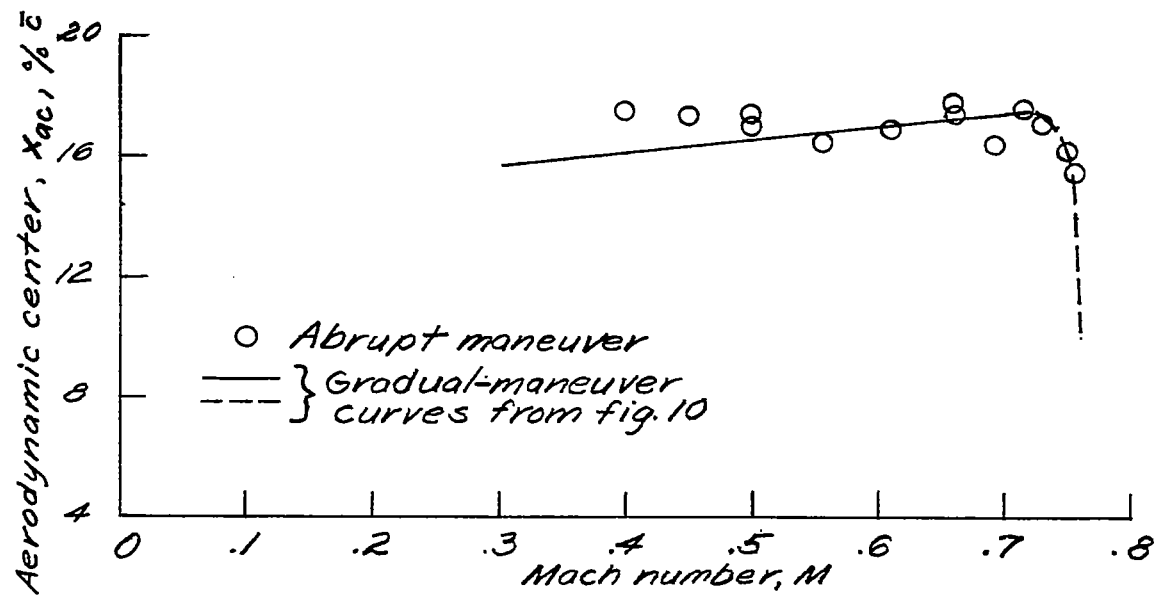

Figure 20.- Wing-fuselage aerodynamic-center position for configuration A in abrupt maneuvers in lower C_{N_A} range.

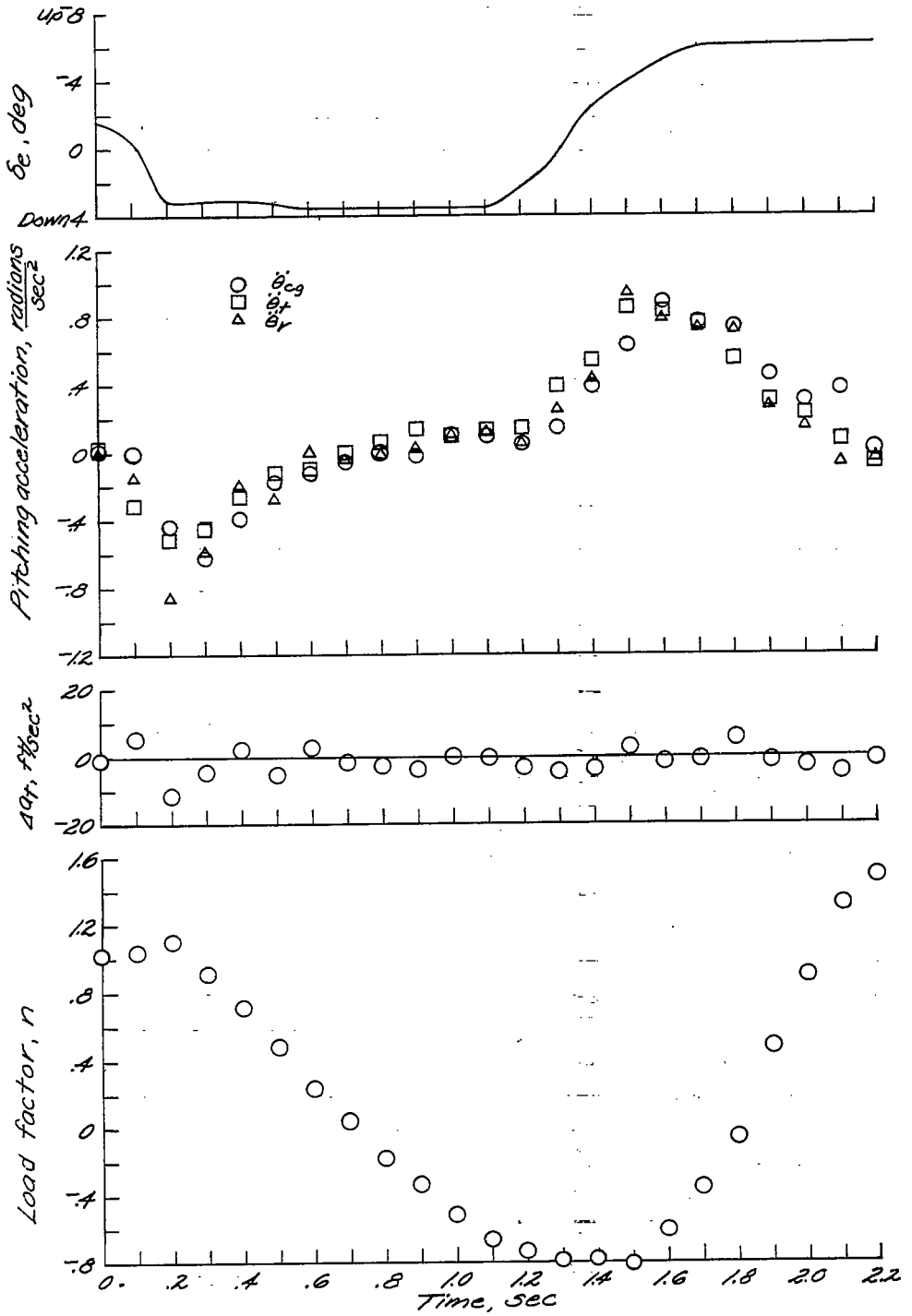

Figure 21.- Time histories of measured quantities and calculated errors of fit in an abrupt push-down pull-up at M = 0.44. Configuration B; h_p = 20,000 feet.

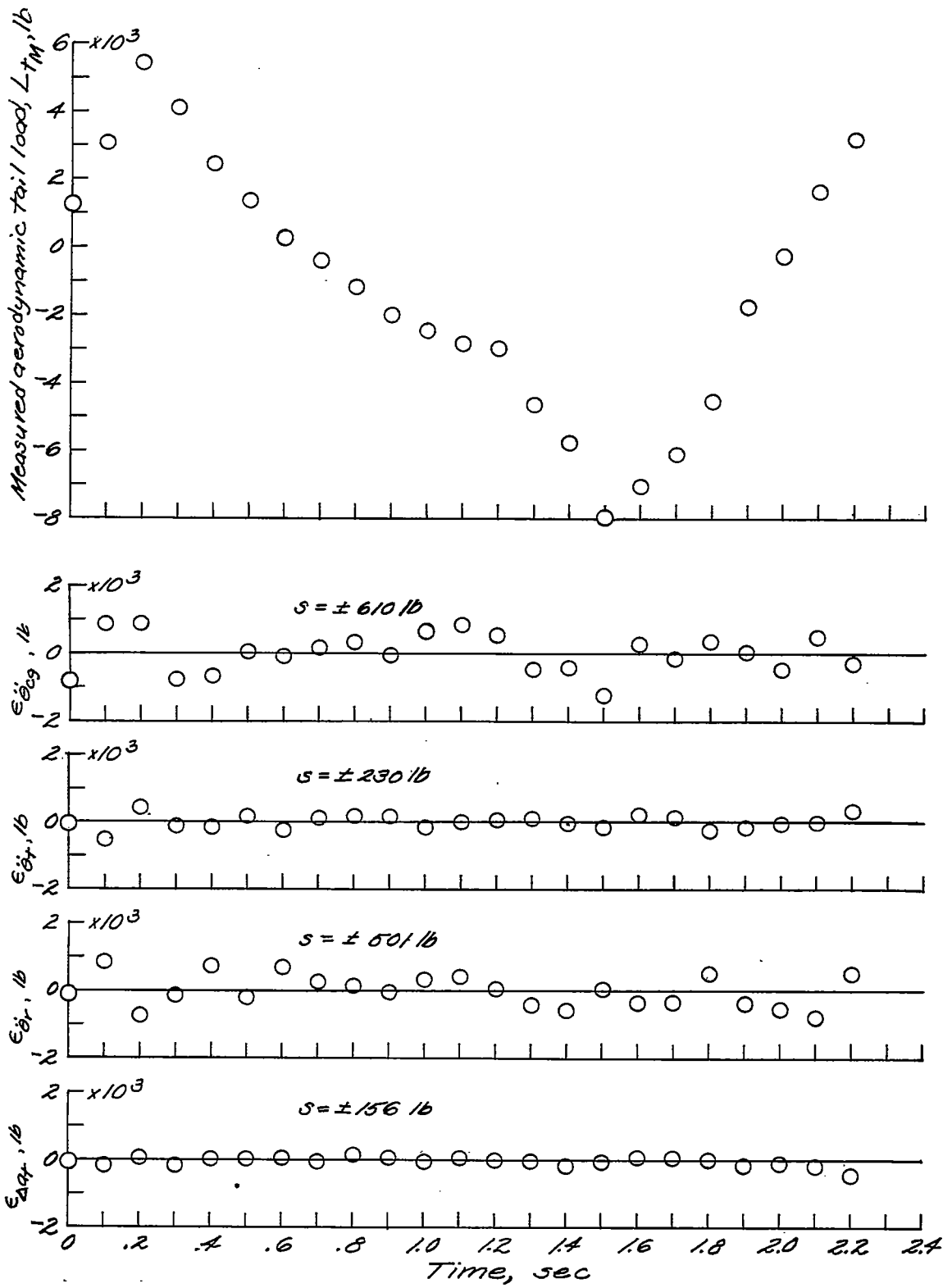

Figure 21.- Concluded.

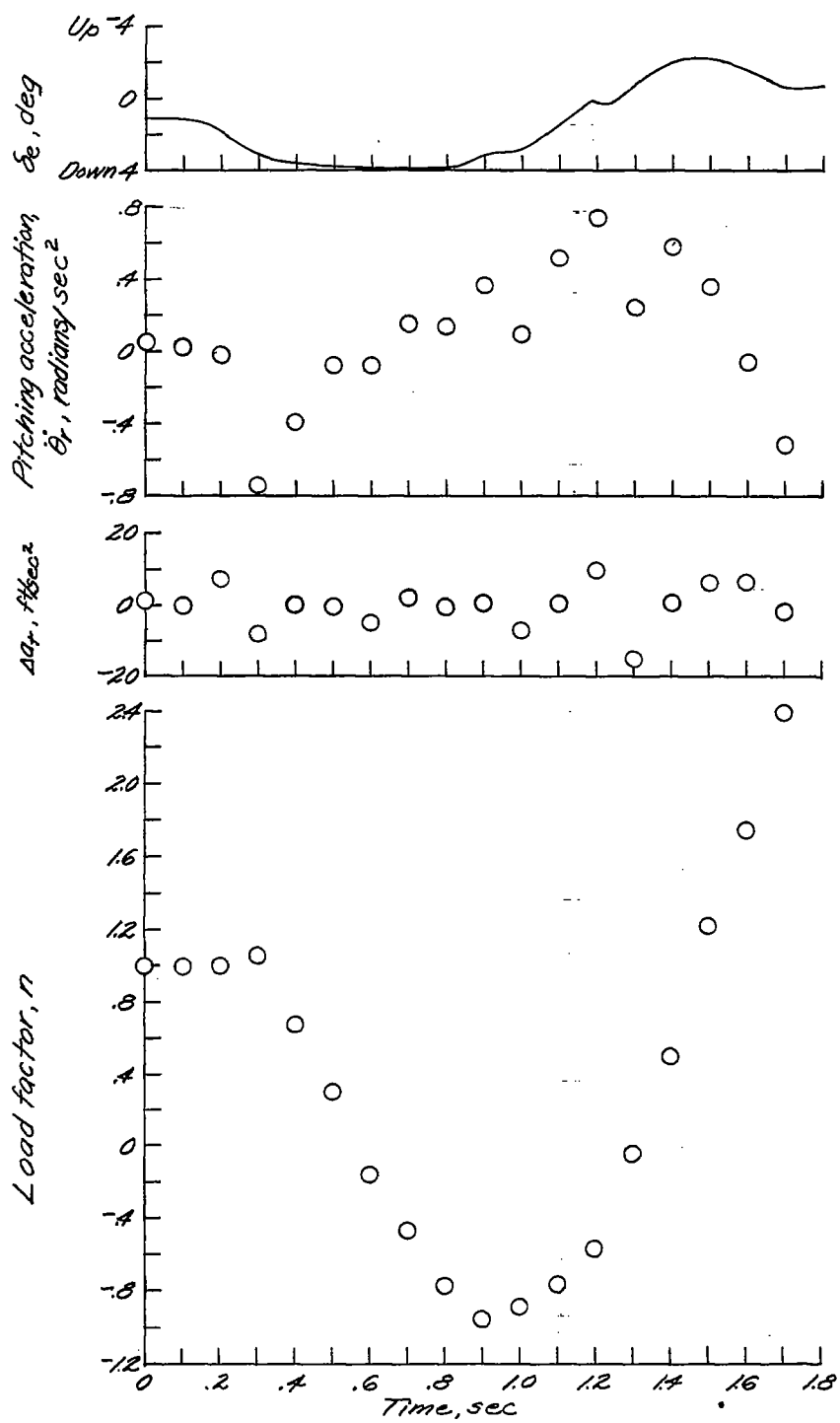

Figure 22.- Time histories of measured quantities and calculated errors of fit in an abrupt push-down pull-up at M = 0.70. Configuration B; h_p = 20,000 feet.

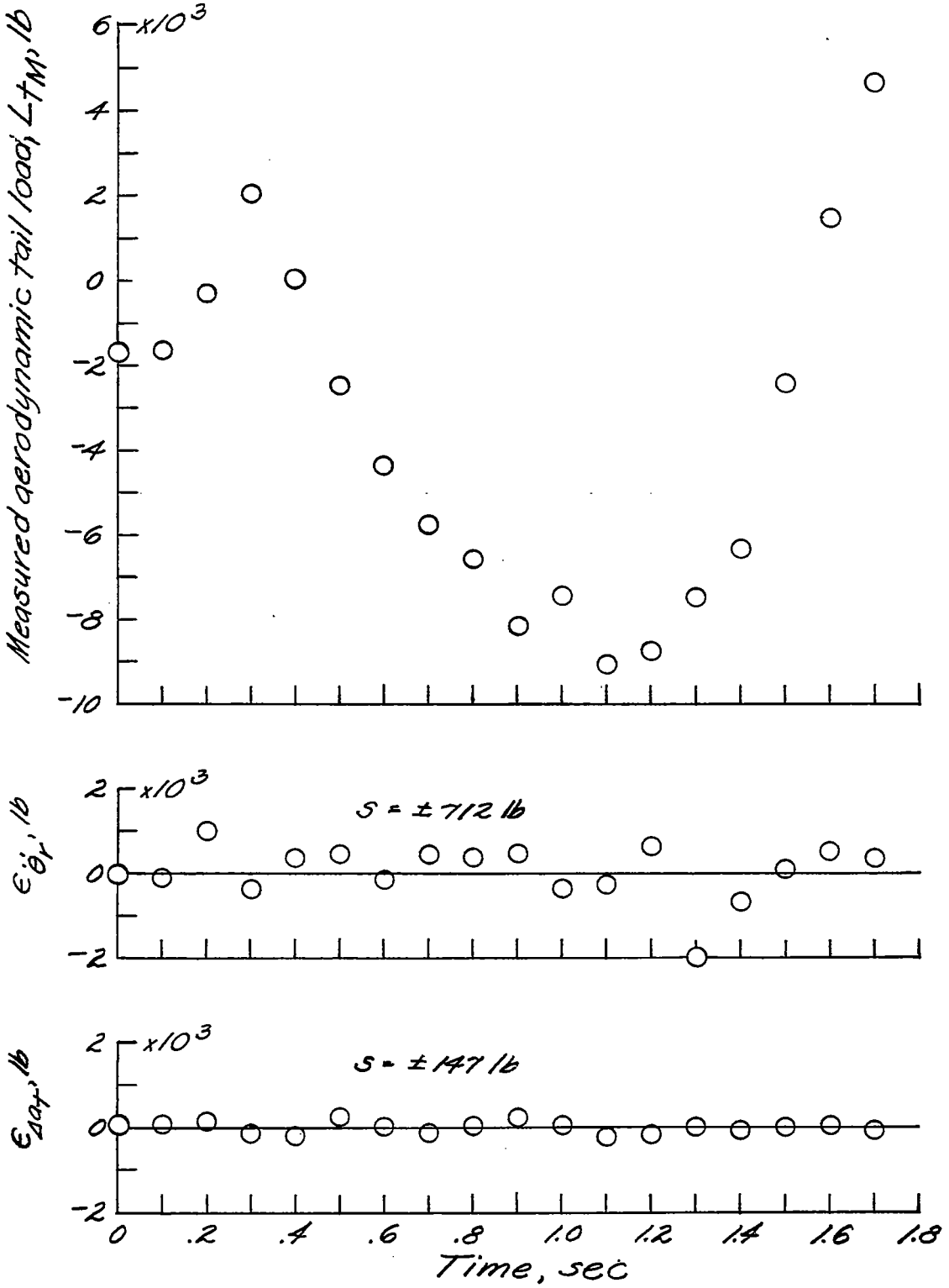

Figure 22.- Concluded.

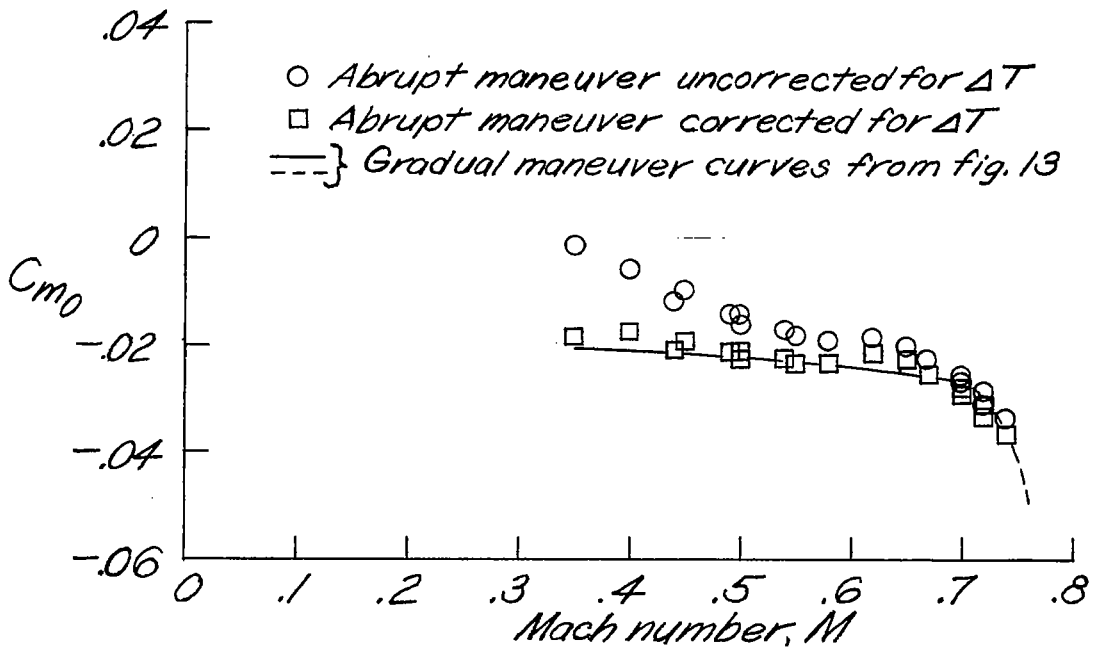

Figure 23.- Wing-fuselage zero-lift pitching-moment coefficient for configuration B in abrupt maneuvers in lower C_{N_A} range.

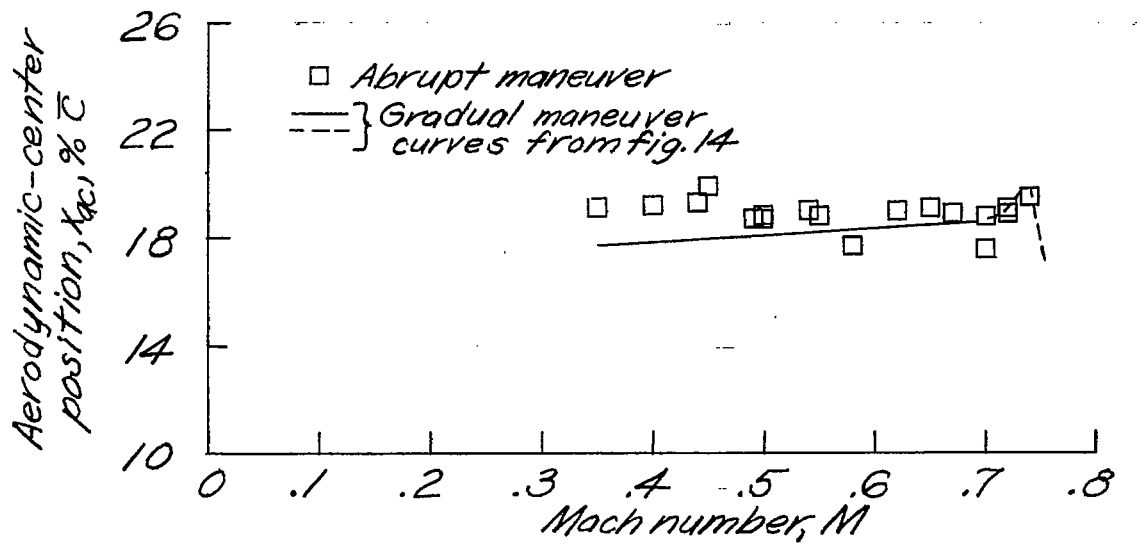

Figure 24.- Wing-fuselage aerodynamic-center position for configuration B in abrupt maneuvers in lower C_{N_A} range.

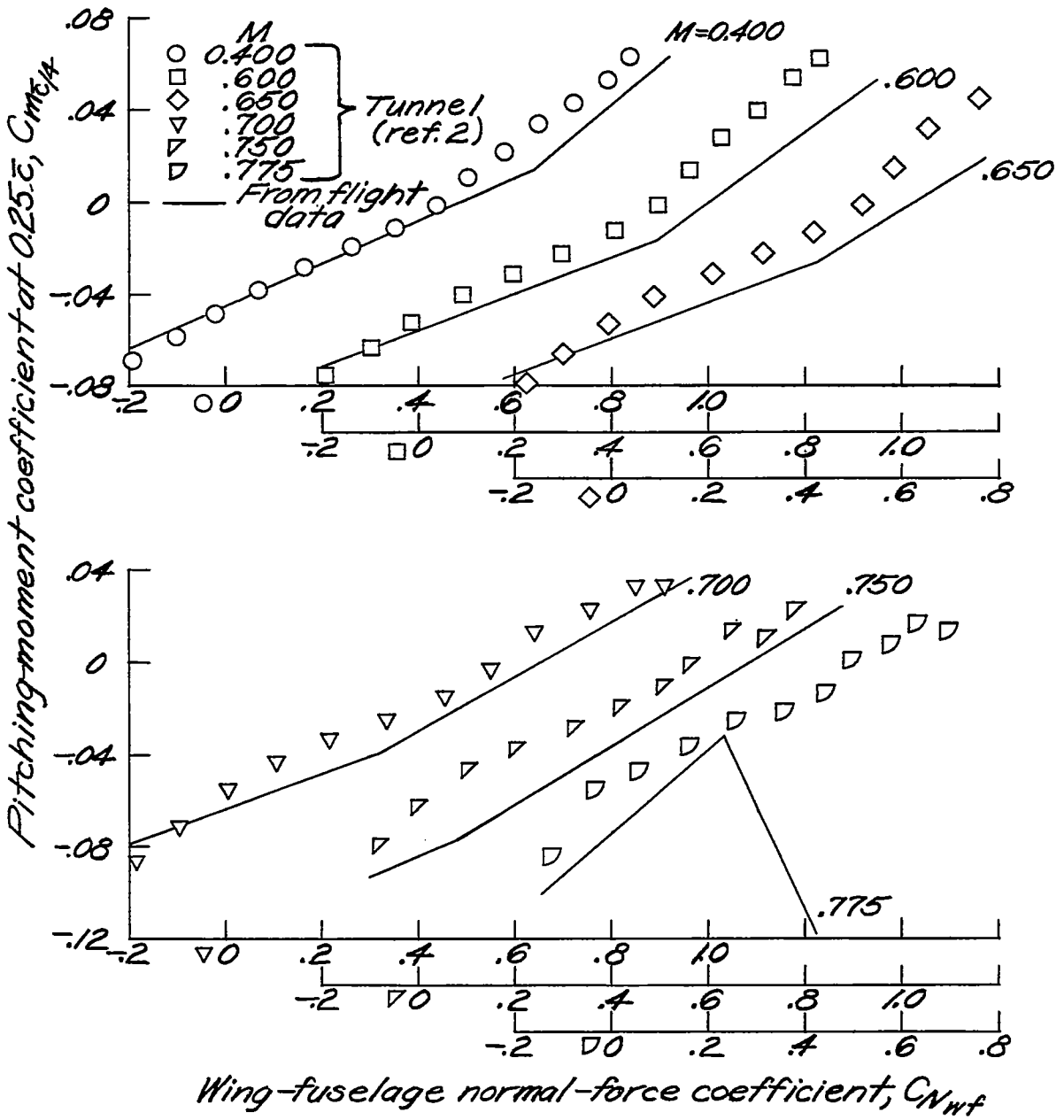

Figure 25.- Comparison of flight and wind-tunnel pitching-moment data for configuration A.

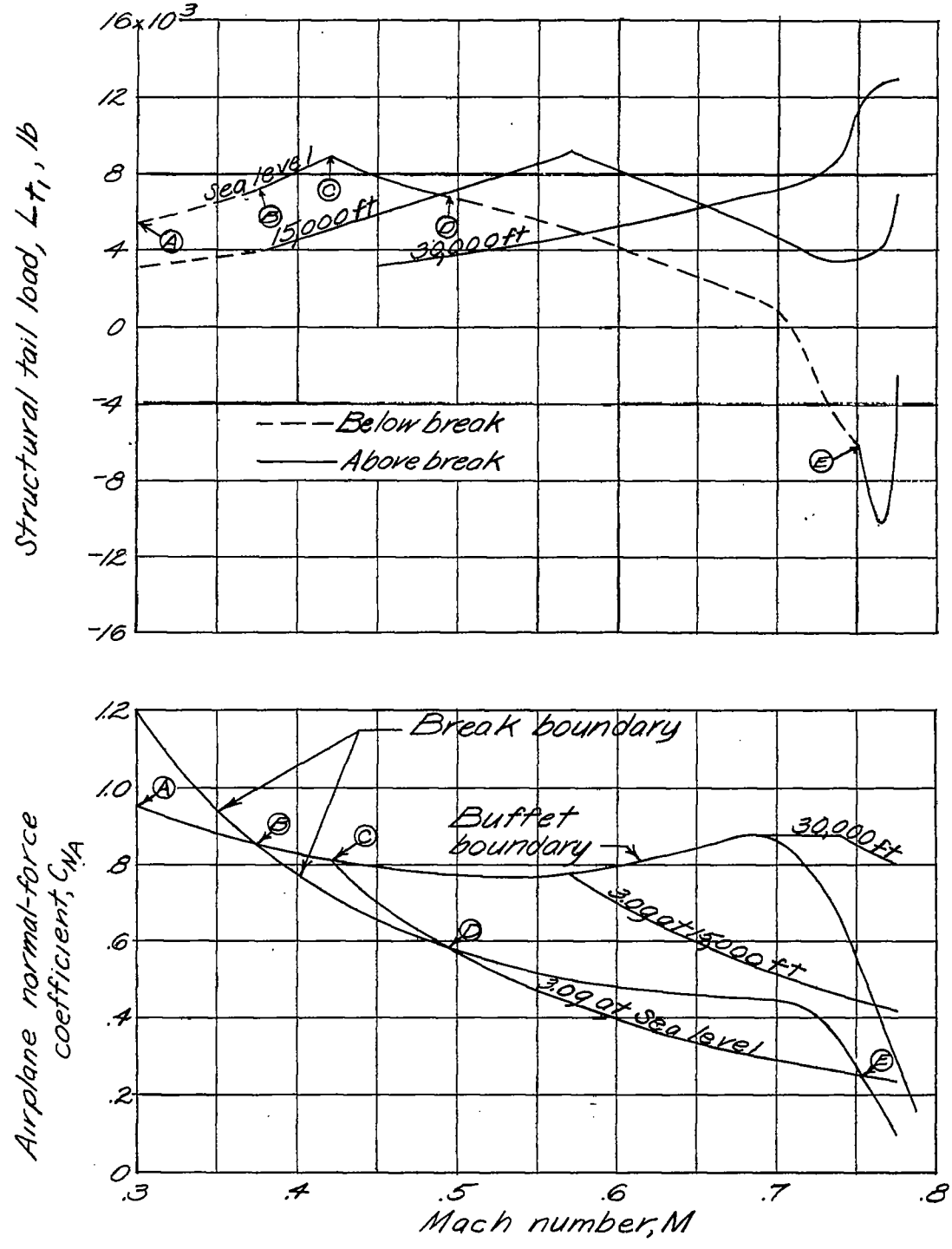

Figure 26.- Calculated structural tail loads and associated airplane normal-force coefficients for North American B-45A airplane for balanced conditions at n = 3.0g or stall. Design gross weight of 82,600 pounds; center of gravity at 32 percent $\bar{c}$.

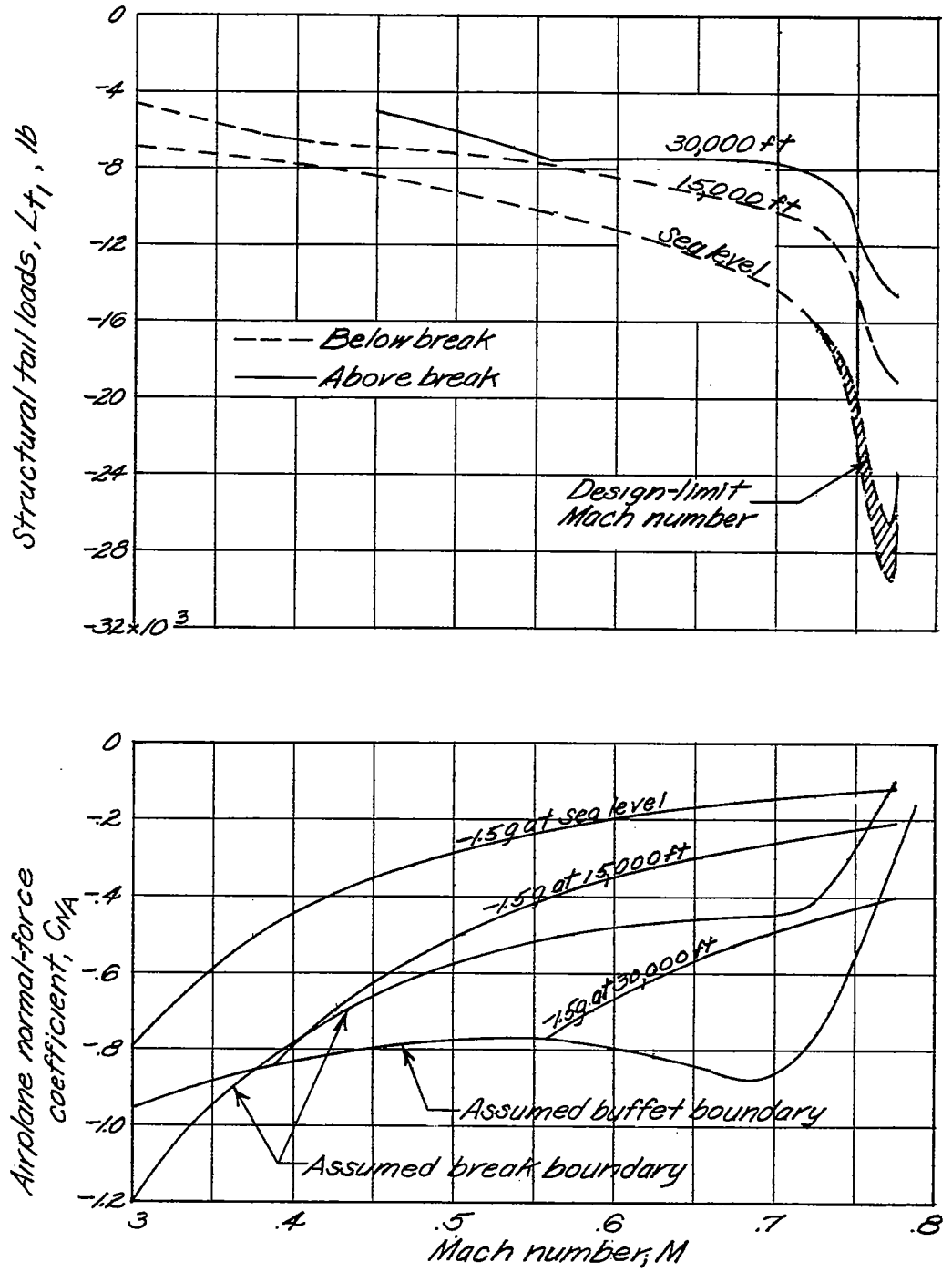

Figure 27.- Calculated structural tail loads and associated airplane normal-force coefficients for North American B-45A airplane for balanced conditions at n = -1.5g or stall. Design gross weight of 82,600 pounds; center of gravity at 32 percent $\bar{c}$.

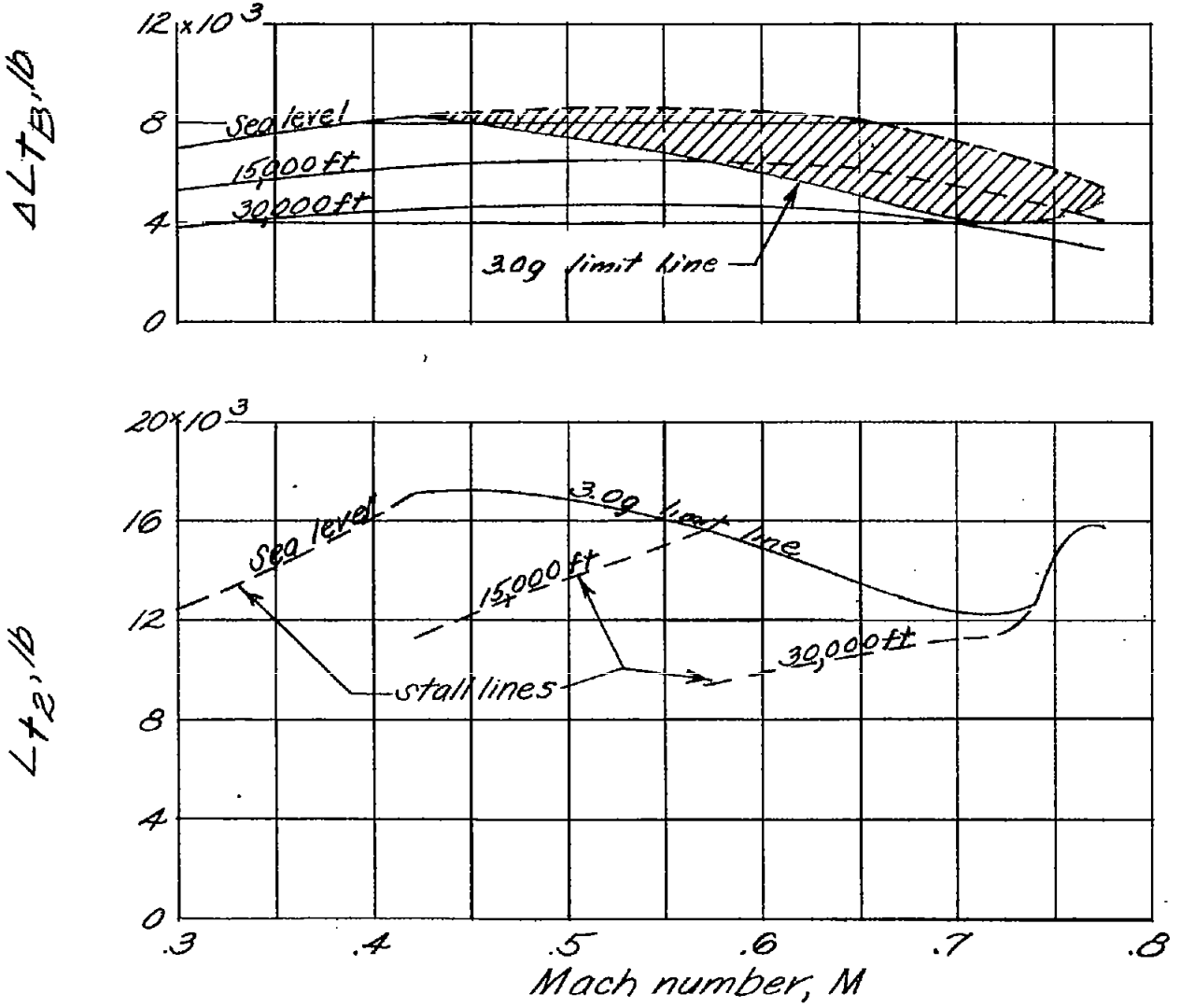

Figure 28.- Buffeting tail loads and maximum positive structural tail loads for North American B-45A.

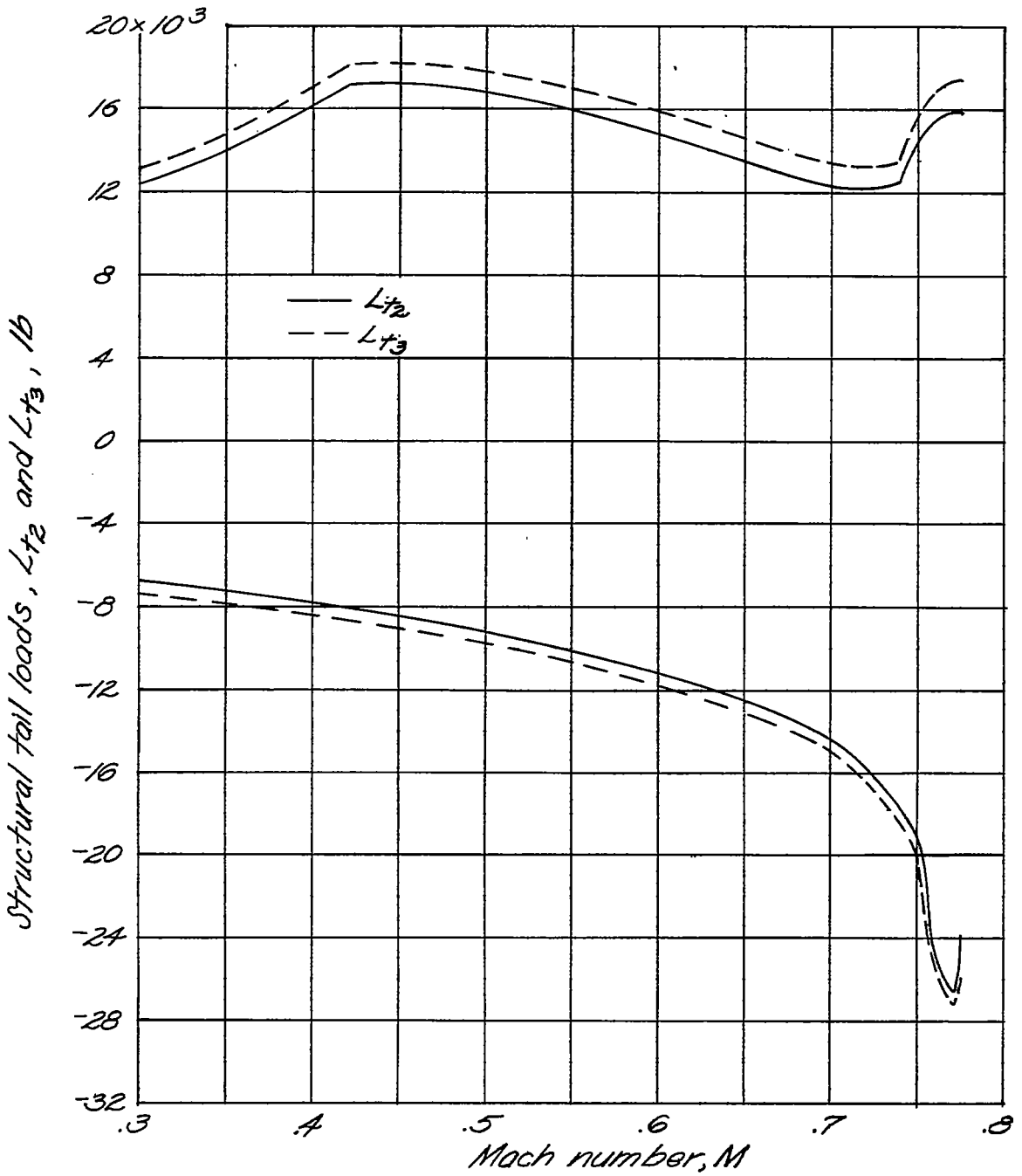

Figure 29.- Structural tail loads L_{t_2} from figures 27 and 28 and structural tail loads with corrections for pitching moments due to trim elevator angle and thrust L_{t_3}.